ICES CM 2004/Poster R:39

Acoustic backscatter from zooplankton and fish explored through an optimized model framework

A. Lebourges-Dhaussy, T. Knutsen, R. J. Korneliussen

Abstract

The purpose of this work has been to test complementary methods in order to classify marine organisms, with particularly attention to zooplankton and fish. Algorithms to separate fish and zooplankton have been developed and implemented at IMR and at IRD. A novel optimised model framework based on known scattering models are used to classify zooplankton and to separate these from fish. Acoustic data from up to 6 frequencies were collected to test the scattering model framework, while concurrent biological samples from multi-net oblique or horizontal MOCNESS tows, WP2 vertical net hauls and pelagic trawl were also obtained and analysed. Great attention are given on one side to the inter calibration and the comparability of all the frequencies, and to the space and time coherence between the samples collected and the acoustical data which are processed. All algorithms involve zooplankton scattering models, the high-pass ones from Stanton, or the more complex ones like the truncated fluid sphere from Holliday or the DWBA set of models from Chu and Stanton. A set of reliable acoustical and biological data has been chosen in order to proceed to comparisons between the results of the acoustic data processing through the classification algorithms and the results of the biological processing.

Key words: categorization, zooplankton, modeling, multi-frequency acoustics

A.Lebourges-Dhaussy, Centre IRD de Bretagne, US (004) ACAPPELLA, BP 70, 29280 Plouzané (Acoustique-halieutique), France [tel: +33 2 98 22 45 05, fax: +33 2 98 22 45 14, e-mail: Anne.Lebourges.Dhaussy@ird.fr]. R. J. Korneliussen and T. Knutsen, Institute of Marine Research, P.O. Box 1870, 5817 Bergen, Norway [tel: +47 55 23 85 00, fax: +47 55 23 85 84, e-mails: rolf@imr.no, tor.knutsen@imr.no.

Introduction

In boreal and sub-Arctic oceans pelagic calanoid copepods and krill are probably the most important organisms transferring primary production to higher trophic levels (Wiborg, 1954; Østvedt, 1955; Melle, 1998). Therefore, there has been a substantial focus over the years to study the abundance and distribution of these organisms at particular localities, for regions and on large basin wide scales (see Hirche et al., 1994; Melle, 1998; Dalpadado et al., 1998; Siegel, 2000a, b). Much effort has also been exercised to improve the sampling methodology for these groups using also new optical and acoustical techniques in order to improve biomass and production estimates and to obtain an improved understanding of spatial and distributional variability (Pieper and Holliday, 1984; Simard et al., 1986; Herman, 1988, 1992; Simard. and Mackas, 1989; Holliday, 1992; Herman et al., 1993; Melle et al., 1993; Stanton et al., 1994; Kaartvedt et al., 1996; Torgersen et al., 1997; Harris et al., 2000; Halliday et al., 2001; Korneliussen and Ona, 2002, 2003**;** Wiebe et al., 2002; Wiebe and Benfield, 2003).

In the present work the potential for detecting these zooplankton groups by multiple frequency remote acoustic techniques has been particularly addressed. During the last decades substantial effort has been undertaken to explore acoustic methodology to determine zooplankton abundance and distribution (Greenlaw, 1977, 1979; Johnson 1977; Holliday and Pieper, 1980; Pieper and Holliday, 1984; Kristensen and Dalen, 1986; Holliday et al., 1989; Sameoto et al., 1993; Cochrane et al., 1991; Benfield et al., 1998). To enhance our understanding of zooplankton backscattering characteristics, increasingly refined mathematical scattering models (Stanton, 1989; Stanton, 1990; Stanton et al., 1994, Stanton and Chu, 2000), as well as more complex and realistic approaches have been developed (Francis, 1993; Francis et al., 1999). The backscattering cross section predicted by these models usually depends on acoustic frequency, size, shape, angular orientation, as well as the sound speed and density contrast between the organism and seawater. The main purpose of this paper has been to explore the potential of multiple frequency acoustic data analyzed by an optimized scattering model framework that includes several of the scattering models pointed to above, both to classify some coarse zooplankton taxa and to separate these from fish detections.

Materials and Methods

Sampling gear

Two types of zooplankton sampling gear were used during this study. These were the multiple opening and closing net system; the $1m^2$ MOCNESS Wiebe et. al. (1976, 1985) and the WP-2 net (Anon, 1968). In the MOCNESS (Multiple Opening / Closing Net and Environmental Sensing System), nine nets are stacked vertically one above the other and open sequentially with one net opening as one is closed. Net 0 is however open when the gear is deployed and closes as Net 1 opens. The MOCNESS sampler was operated with 180 μm meshed nets and towed obliquely with net sampling at predetermined depth intervals or horizontally in particular scattering layers as determined from the real time acoustic displays. It was equipped with pressure and tow angle sensors and flowmeter, and the signals were transferred via

conducting cable to the deck unit onboard the ship. A computer program in the PC controlling the deck unit calculated the volume filtered and recorded the depth interval for each net. The WP-2 net used in this study was of 180 μm mesh size and was vertically lowered at 60 m min^{-1} and retrieved at 45 m min^{-1} as recommended (c.f. Anon, 1968). Depths sampled were normally from 0 to 100 m or 0 m to the bottom.

General laboratory procedures

The samples obtained with MOCNESS and WP-2 nets were treated and worked up according to standard IMR procedures for mesozooplankton sampling. First, each sample was usually divided in two parts, one for biomass estimation and the other for species identification and enumeration. The samples for species identification were stored on 100 ml flasks and fixated to a 4 % formalin and seawater solution for later species identification in the laboratory. The biomass part was size fractionated using sieves of 2000 μm, 1000 μm and 180 μm mesh size, hence giving biomass size fractions >2000 μm, >1000 μm and < 2000 μm, and >180 μm and < 1000 μm. The biomass samples for each size fraction were put on pre-weighed aluminum dishes and put in an oven at 60 ^{0}C for drying approximately 20 hours onboard the research vessel. Upon drying the samples were stored in a freezer at –20 ^{0}C for the remaining part of the cruise. On returning to the laboratory at IMR they were further dried in a laboratory oven at 60 ^{0}C for 3 hours. In addition fish, krill and shrimps from the biomass size fraction >2000 μm were counted, weighed and their lengths individually measured and species identified. In some cases, these groups were also picked out from the complementary part prior to formalin preservation and included with the specimens for biomass determination. These measurements were done to the nearest mm by placing the individuals onto plastic-covered mm-paper.

Taxonomic analyses

Selected samples from MOCNESS and WP-2 have been analysed at the Institute of Marine Research, using their routine procedure for zooplankton taxonomical analysis.

This includes identification to species or genus for most plankton groups, with separate enumeration of copepodite stages for *Calanus* spp. and some other calanoid copepods. For krill, amphipods and pelagic gastropods the most important species were identified and sized to predefined size categories, while some important mesopelagic shrimps and medusae were identified to genus and sized to relatively coarse size classes. Subsampling was used in an adaptive manner depending on the abundance of specimens in the samples. Large and less abundant forms (e.g. krill, amphipods, decapods, chaetognaths, ctenophores and fish) were often counted in the whole sample. Medium-sized organisms (e.g. *Calanus* copepodites) were counted in from ½ to 1/64 fraction. Small organisms (e.g. small copepods) were counted in from ¼ to 1/512 fraction. The degree of subsampling was adapted so that in most cases more than 100 individuals of the most common species or groups of medium and small organisms were counted.

For some groups, particularly the physonect siphonophores (having an apical gas filled pneumatophore), their special morphology and fragile colonial structure, makes

it difficult to analyse this group in a quantitative manner as the colony often breaks apart upon capture in the nets. This also holds for siphonophores that lack an apical pneumatophore but possess at least 1 relatively large swimming bell (Order Calycophora). Direct identification and enumeration onboard the research vessel using freshly caught material, should possibly to be preferred. It seems, that fragile parts of these colonies do poorly withstand formalin fixation, and/or handling related to the standard procedures for zooplankton analysis. Qualitative inspection of fresh samples gave some coarse information on their occurrence, and notes were made on their presence in the original zooplankton sheets during working up the samples at sea.

Measurements of zooplankton size

Some measurements of individual zooplankton size were conducted during the course of the laboratory analysis at IMR based on the preserved part of the samples. This complement the individual measurements conducted at sea on macrozooplankton from the biomass fraction (see above) and the coarser size classification following species identification. However, earlier measurements have additionally been used, where such have been needed. During the ICES Sea-Going Workshop in 1993, morphometric measurements were carried out on a number of zooplankton taxa in samples obtained from the upper 100 m with MOCNESS (Wiebe et al., 2002). The measurements included length and width and/or height, for the various taxa. The measurements were originally carried out using a binocular microscope at 40X magnification. In addition a quite extensive set of morphometric measurements of zooplankton as reported by Halliday (2001) have been used when applicable. This work includes a.o. the comparison of morphometric and geometric methods for the estimation of individual zooplankton volumes, which is relevant to the calculation of the Equivalent Spherical Radius (ESR) or Equivalent Radius (ER) needed for comparing model data with measured zooplankton size and abundance.

Acoustic sampling

Collection of acoustic data was guided buy the recommendations in Korneliussen et al. (2004). Acoustic data was collected with an EK500 Simrad scientific echsounder with transducers mounted in a drop keel on RV G.O. Sars in October 2002 in the North Sea operating with 4 frequencies; 18, 38, 120, and 200 kHz. In October 2003 the new Simrad EK60 was used to acquire raw data at 6 frequencies; 18, 38, 70, 120, 200 and 364 kHz, using the new research vessel of IMR that replaced the old RV G.O. Sars, hence obtained the same name from the date of replacement. Additional biological data obtained by a pelagic trawl (c.f. Valdemarsen and Misund, 1995) and acoustic data acquired with RV Johan Hjort during a capelin cruise in the Barents Sea in September 2003 using the following transducers frequencies; 18, 38, 120 kHz (drop keel mounted) and 200 kHz (hull mounted some meters away from the keel mounted transducers). All echo sounder systems were calibrated according to Foote (1982), and Foote et al., (1987). The calibration of the EK60/364kHz system was not optimal, possibly due to connecting the electronic part to wideband (120 kHz) transducer resonant at 400 kHz. The volume backscattering data, sv, from the EK60/364kHz-T400kHz system can still be used with some care. During logging of raw data with EK60, the function to additionally store acoustic data in BEI Big Endian format was

used, hence EK60 generated data that could also be read by the BEI post-processing system (c.f. Foote et al., 1991; Korneliussen, 2004).

The files used by BEI hold data from each frequency in separate files normally based on a sailed distance of 5 nautical miles. All collected acoustic data were corrected for noise (Korneliussen, 2000) prior to further processing. In order to exchange data between Simfami partners and import the 4 or 6 frequency acoustic data to Movies+, Echoview and other postprocessing applications, all relevant acoustic data from the IMR cruises in 2002 and 2003 were converted to the HydroAcoustic Common format (HAC[1]) (c.f. Simard et al., 1997, 1999). This was achieved by an application called **bei2hac** developed at IMR (Knutsen, in prep.). Inherent in the HAC format specification, data from all logged frequencies should be stored sequentially in one file as volume backscattering strength (Sv), the size of the files being determined either by the producing application itself or interactively by the user on execution.

All "raw" EK500 ping data and EK60 sample data were recorded and ultimately stored on tape and DVD's. During the cruise many gigabytes of data were acquired. These data were processed in near real-time using the Bergen Echo Integrator (BEI), particularly targeting the mackerel *Scomber scombrus* as a key species. Ultimately the scrutinized data was entered into an Ingres database system, which normally forms the backbone for further processing.

However, for the present work volume backscattering strength (Sv) data from the HAC files were extracted by the help of the Simfami database (Gajate et al., 2004), where information on net hauls and pelagic trawls are stored and also overlaid as polygons on images of the acoustic registrations.

[1] HAC = HydroACoustic common data exchange format as recommended by ICES WG FAST.

Multifrequency classification processing

For the acoustic multifrequency processing purpose, the first step has been to realise an echointegration by layers on the raw data, at the six frequencies, with an integration threshold of –80 dB. For this purpose the software Movies, designed by Ifremer (Weill et. al. 1993), has been used. Small integration cells were defined in order to come as close as possible to a situation where one type of organism dominates the acoustic reflection. According to the maximum number of integration layers allowed in the post-processing software (40 in Movies+) and to the maximum range of interest for each orignal data file and corresponding plankton station, the height of the layers varies between 2 and 3 meters. The distance unit of integration (ESU) is 30 pings At a ship speed of 2 to 3 knots and with about 1.5 second between pings, this corresponds to a horizontal distance of about 55 m (Figure 1). To have a geographic and time coherences between the plankton sampling and the acoustic data, the integration has been performed in accordance with the polygons as outlined in the Simfami database showing the localization of the MOCNESS tows, the WP2 net and trawl samples.
The input data for the multifrequency classification processing are the measured mean volume backscattering strengths (S_v) at the various frequencies for each integration cell, thus in this case at the six frequencies: 18, 38, 70, 120, 200 and 364 kHz.

Because of the strong absorption of the 364 kHz, no layer below 130 m was considered

The main principles of the classification algorithm are described in Greenlaw (1977, 1979), Greenlaw & Johnson (1983), Pieper & Holliday (1984). These techniques were originally developed for mesozooplankton classification, like the copepods, hence to process very high frequencies data (from 265 kHz to 3 MHz). The purpose here is to apply an expanded algorithm compared to the previous approach. The aim of the expansion is to design a classification tool that also allows classification of larger zooplankton organisms from the frequencies of the classical echo sounders (18 to around 400 kHz). The models incorporated into the overall algorithm framework are comprised of a set of models available in the literature for the main groups of zooplankton:

- the **copepods** with: the truncated fluid sphere (Holliday, 1992), the Stanton's (1989) high-passes fluid sphere, fluid prolate spheroid, the DWBA models of fluid ellipsoid ;
- the **euphausiids** with: the Stanton's (1989) high-passes fluid bent cylinder, the Stanton & Chu (2000) DWBA models of fluid bent cylinders for small and for large euphausiids, the density contrast and the compressional speed of sound contrast "g" and "h" respectively being different;
- the **gastropods** with: the Stanton et al.'s (1994) high-pass elastic shelled model.

Models of **gas bubble**, for zooplankton with gas inclusions, are included also with:

- the Stanton's (1989) high-pass gaseous sphere, and the Chu (pers. com.) DWBA model of gaseous sphere.

At this stage the model introduced for a **swimbladder** is only the Stanton's (1989) high-pass gaseous prolate spheroid, which is of course very rudimentary. At least it can fit situations where there are very low variations with the frequency.

Another paper at this ICES annual 2004's conference, describes the details of the algorithm framework and gives the results of simulations that have been performed on virtual populations (Lebourges-Dhaussy and Ballé-Béganton, 2004). These simulations help to understand how the processing depends on various input parameters, how to make optimal choices for the settings of these parameters and the selection of models for field data applications. In the present paper only a simple description of the processing is given. The starting point is the hypothesis of linearity concerning the construction of the scattering, saying that the volume backscattering strength is the linear combination of the contributions of each organism present in the scattering volume, expressed mathematically as:

$$s_v(\text{freq } j) = \text{sum on } i \ (Ni * \sigma_{bs} (\text{size } i, \text{freq } j)) \qquad (1)$$

σ_{bs} being the backscattering cross-section of a single target organism. This is estimated from a scattering model fitting a particular type of organisms (c.f. copepods, euphausiids, gas bubble, …) that is thought to dominate the reflection in the volume considered. The size of the organism (understood as an equivalent radius)

and the frequency applied, are the most influent parameters on the models, but other important parameters are the density contrast, “g”, as well as the sound speed contrast, “h”, between the organisms and their surrounding medium. Nevertheless these two parameters are fixed inputs in the software. Each model has its adjusted values; they are merged in Table 1. Ni is the abundance (number of individuals) of organisms of the size i.

With as many of such equations as there are frequencies, the problem is expressed in the present case as a system of six equations of the type of (1).
The size is understood in terms of equivalent radius, whatever is the model shape (sphere, cylinder, ellipsoid).
The S_v (that is $10*\log(s_v)$) are the measurements, the frequencies are known.
The inputs are the initial, given *a priori* by the user and the choice of models, chosen also by the user. The size vector is improved through iterations allowing keeping the sizes that have non-null abundances, building a new size vector on which a new resolution of the problem is made (Lebourges-Dhaussy, 1996).
The unknown parameters are the abundances Ni, which are the outputs of the processing. The resolution of the system through an inversion is made from the Non Negative Least Squares algorithm.

Prior to the processing of the IMR’s data by the classification algorithm, several simulations were performed on virtual populations, including sizes comparable to the sizes of the organisms sampled with the nets (Tables 2 to 5; Halliday, 2000; Wiebe et al., 2002). A set of simulations has helped to derive optimal settings for internal parameters of the algorithm (degree of underdetermination of the problem and Levenberg-Marquadt (Lawson and Hanson., 1974) parameter allowing the processing to force a type of solution). Another set was more targeted on the initial size vector according to the sizes present in the detected population; it helped to define the conditions for the best model recognition, biovolume estimate and sizes extraction. The virtual populations profile has been build from a set of size vectors of 20 random sizes included between 0.05 and 7 mm for organisms fitting the fluid (sphere, prolate spheroid, bent cylinder) and elastic shelled models and also the gaseous sphere. A populations’ profile of “swimbladders” was also build from the high-pass gaseous prolate spheroid model and from a set of size vectors included in the [1 15] mm range. Several size ranges have been tested for the initial size vector of the processing: [0.01 5]-[0.02 5]-[0.02 10]-[0.05 10]-[0.05 5]-[0.1 10]-[0.1 20]-[0.5 30]-[0.2 15] mm. For three of these size ranges ([0.05 10]-[0.1 10]-[0.2 15]), with an under determination of 4 (the abundances are searched for a size vector of 24 sizes if there are measurements at 6 frequencies), no mistake in the model recognition is observed on the tested virtual populations. The best estimates of the biovolume are obtained with the same size ranges. The latter belong also to the set of size ranges giving relatively good estimates of the mean sizes. Therefore the whole processing consists of iterations based on these three size ranges; the results kept are those giving the lowest residual error among the three. The residual error is the norm of the difference vector between the Sv measured and the Sv recalculated from the predicted population (size vector extracted, abundances calculated, model chosen). For the model choices, the time consumption has been also taken into consideration in this application to field data: according to the shortness of the ESUs and the thickness of the vertical layers, each ESU being equivalent to one vertical profile, the processing of a Mocness station of 30 ESUs can take less than 5 minutes if all models tested are high-pass ones, but nearly two hours

if three of the models used are of the DWBA type (on the computers used for this work). The high-pass have thus been retained in this application, but for checking purposes comparisons have been performed for two stations with the results obtained with the DWBA models.

Acoustic data processing results

The plankton stations used for these processing are issued from the IMR 2003' mackerel survey at six frequencies (18, 38, 70, 120, 200, 364 kHz) and one data set from the 2003 capelin survey using the four frequencies: 18, 38, 120, 200 kHz, has also been processed, corresponding to the pelagic trawl station PT557, which gave a substantial amount of krill and some polar cod. The corresponding biological data are presented in Tables 2 to 5. Figures 2 and 3 show the echograms at the six frequencies for the two stations MOC262 and MOC266, after an echointegration on small cells. In Figure 2 (MOC262) there is clearly a decrease of energy from the low to the high frequencies for the whole echogram. For MOC266 a more complex pattern appear with a distinct scattering layer around 80 m depth being stronger at the highest frequencies, while another scattering layer around 25 m depth shows an increase in energy at the lowest frequencies and, in between, different configurations. Considering the other stations, the MOC260, MOC268 are comparable to the MOC262 with respect to the frequency response trend (Figure 4 a, b).
Using the settings determined from the simulations as allowing the best model, size and biovolume recognitions, the algorithm has been applied to these data. The under determination is therefore of 4, the three above-mentioned size ranges are used successively in an iterative process, and the results corresponding to the lowest residual error are kept. The models used were: the truncated fluid sphere model (Holliday, 1992) for the copepods, the high-pass fluid bent cylinder (Stanton, 1989) for the euphausiids, the high-pass elastic shelled (Stanton et al., 1994) for the gastropods, the high-pass gaseous sphere (Stanton, 1989), as for the gas inclusion of a siphonophore, and a high-pass gaseous prolate spheroid (Stanton, 1989), i.e. as a model representing a rudimentary swimbladder.

The main observation that can be seen from the results of this first processing, after optimisation on the range of the initial size vector, is that the gaseous sphere model dominates as soon as there is a strong scattering at 18 kHz compared to the higher frequencies (Figure 5). The corresponding sizes are generally very small (less than 0.1 mm of radius), leading to a solution that is difficult to interpret from a biological point of view. Even if the gas inclusions of the siphonophores might be as small as the sizes determined by the processing, the predominance of this model on the whole echogram seems strange. Actually, when the S_v levels at 18 and/or 38 kHz are much higher than at the higher frequencies, like in the case of the MOC262, a model offering a resonance at 18 or at 38 kHz matches the data well. This is the case for the gaseous sphere model in the size ranges considered (Figure 6). It can be noticed however that the fit between the data and the model solution is all right until around 50 m depth, then not too bad until 75 m, then rather bad below except for the 4^{th} and 5^{th} ESUs. This denotes, even if the closest fit to the data is obtained with the gaseous sphere model everywhere, that the nature of the reflection is different is these three parts of the echogram. The processing of acoustic data corresponding to station MOC260 (Figure 7) also gives a predominance of the gaseous sphere model with very small sizes (equivalent radius –ER- less than 0.1 mm); some cells in the thin layer at 50 m

depth are categorized as gaseous prolate spheroid (in red on the figure) with small sizes also (two main ER classes: 0.05-0.07 mm and 0.16-0.24 mm); two cells are categorized as fluid bent cylinder, the upper one presents very low abundances with equivalent radius of 8 and 16 mm, but the lowest one presents the highest abundances for equivalent radius around 1.26 mm (thus a length around 13.3 mm if length/radius=10.5) and weak presence of ER of 8 mm and 16 mm. Two cells are also categorized as Truncated fluid sphere (TFS) with equivalent radius from 0.6 to 1.1 mm for the highest abundances and presence of larger ER: 4.5-9-16 mm, thus not corresponding to copepods. The three cells classified "elastic shell" present equivalent radius of 2.4 mm for the first ESU and 1.8 mm for the 10^{th} en 11^{th} ESUs. The residual error is rather high in the lowest part of the echogram, between the two thin layers clearly visible at 364 kHz.

Taking into account the presence of high values of the residual error for these two stations, a check has been performed using the DWBA models for the copepods and the euphausiids, in order to verify if more accurate models could fit the data better than the high-pass ones and perhaps allow to recognise better new integration cells. Therefore the processing has been done with the following models: DWBA fluid ellipsoid for the copepods, two DWBA fluid bent cylinder models for the small and the large euphausiids, then the same high-pass models for the elastic shell, the gaseous sphere and the gaseous prolate spheroid. The results are given on Figure 8 a and b. They are identical to the previous ones for MOC262, and for MOC260, the only difference is that there is no more recognition of "euphausiid-like" nor "copepods-like" scatterers, the corresponding cells are classified by the "elastic shell" model, with quite identical residual errors (0.70, 0.74, 0.91 with high-passes models; 0.71-0.79-0.96 with DWBA models). The problem remains the domination of a scattering indicating gaseous-type scatterers.

The results for the stations MOC266 and MOC268, are shown in Figure 9 a and b. For the MOC266 station, the classification is much more complex than for the three other ones. This could be expected, as the frequency response trend is very variable depending of the location in the echogram. The classification process gives stratification between the "copepod-like" and "euphausiid like" models, with elastic shell and gaseous prolate spheroid models more mixed. The mean sizes corresponding to the cells recognised as truncated fluid sphere model are often too large to be copepods (from 3.5 to 6 mm and in some places around 1 mm); corresponding to the fluid bent cylinder model, the mean sizes estimated can be around 0.5 mm and 5 mm; the elastic shelled model is related mainly to mean sizes around 1 mm. The station MOC268 is simpler; there is however an area around 100 m where the algorithm classifies as "euphausiid type" scatterers and more dispersed points with "copepod type" scatterers. For these two stations, as for the two previous ones, the accuracy in terms of norm of the residual error is not satisfying, even for the MOC268, which is globally the best one from this viewpoint.

In order to look for improvements in the residual errors (which have been mostly above 0.5 until now (c.f. Figure 12) and also to check the variability of the result according to the frequencies involved, additional processing was performed without the 18 kHz, without the 364 kHz and without both.
It is clear that suppressing the 18 kHz results in more classification as fluid and elastic like organisms, where it was categorized as gaseous previously (Figure 10). The

algorithm now classifies as "truncated fluid sphere" a large part of the integrated cells below 70 m depth for the MOC262 station. For a part of them they are related to mean sizes around 2 to 3 mm; for a large other part they are estimated with mean sizes of 17 mm. For the station MOC260, the classification now suggests the presence of copepods and large fluid sphere like organisms (mean sizes around 2.5mm, 6mm, 15mm), appearing mainly in a layer around 100 m depth (visible in Figure 4a on the 200 kHz echogram). Around 50 m depth, the elastic shell model solution (mean sizes around 2.5 mm) has replaced a part of the gaseous prolate spheroid model solution. The same is found for the station MOC266, where for some cells in the upper part of the echogram the gaseous sphere model is replaced by the TFS, fluid bent cylinder and elastic shell models. The mean size estimates for the fluid-like and elastic-like models remain among the values: 1, 3, 4 and 6.5 mm. At the same time, for this latter station, there is some improvement in the residual error, while it is not the case for the two other stations. There are also some improvements on the error for the station MOC268; here still more cells fit the TFS, elastic shell and fluid bent cylinder models, with mean sizes around 2.5, 7, 15mm, mainly below 80 m depth but also shallower.

Suppressing the 364 kHz in the processing gave only minor changes in the model recognition compared to the processing with the six frequencies, and no change at all for station 262. For station 260, one cell classified as “TFS” changed to “fluid bent cylinder” and a few cells changed from the “gaseous sphere” type to “gaseous prolate spheroid. For station 266, practically all “TFS” classified cells were re-classified to “euphausiid like” or “gastropod like” organisms (mean sizes in the 2 to 5 mm range); the gaseous sphere model is chosen in cells where it was previously categorized as fluid bent cylinder in the upper part of the “complex” layer. For station 268, the fluid and elastic model solutions has disappeared leaving only gaseous sphere and a few prolate spheroid. The clear difference between the processing with the six frequencies and the processing without the 364 kHz is however a strong improvement in the residual error (c.f. Figure 11). This is particularly evident below 50 m depth for stations 260 and 262, but appears more evenly distributed for stations 266 and 268.

The last processing has been made without 18 and 364 kHz. The population solutions obtained are simpler than when only 18 kHz was suppressed, leading to a 364 kHz imposing conclusive constraints, for example to reveal differences between the two fluid model solutions (Figure 13). Now there are more cells classified as fluid bent cylinder for stations 266 and 268. In the case of a quite uniform decrease of the scattering from 18 to 364 kHz, like in station 262, the gaseous sphere model remains the model uniformly recognized. In the case of station 260, Figure 4a shows the decrease of the scattering intensity with frequency, but the stronger steps are from 18 to 38 kHz and 200 to 364 kHz. The gaseous sphere model remains dominant but as the extreme frequencies (18, 364 kHz) are not considered, the algorithm classifies more integration cells as “gaseous prolate spheroid” than with the six frequencies, as this is a rather flat model in the “ka” range corresponding to a 38-200 kHz range and a 0.1-10 mm size range. For the four stations, what is strange, the very top of the echogram is classified mostly as truncated fluid sphere, with a residual error quite high.

Processing the data corresponding to the pelagic trawl 557 (PT557) was interesting for several reasons. The catch was composed of a large majority (in weight) of krill but contained also swimbladdered fish, and it has been registered by the four classical frequencies: 18, 38, 120 and 200 kHz (Figure 14). The whole echogram has been

processed by the classification algorithm framework, in order to analyse the region where swimbladder fish probably dominate. The duration of one processing was too long (several hours) to allow an optimisation on several size intervals, thus the run has been done in the [0.05 10] mm size range. The algorithm classified the layer just above 150 m depth with the fluid bent cylinder model, mixed with some truncated fluid sphere model (mean sizes from 0.7 to 2.6 mm) (Figure 15). In this case, the sizes estimated can be coherent with the presence of krill. The residual error remains below 0.5 in rather this entire depth layer, which is quite satisfactory. All the rest of the echogram appears as gaseous sphere of very small dimensions, but even if the residual error is low, this result does not seem be very realistic This is the reason why a final processing was performed with only the gaseous prolate spheroid as the active model and the size range a bit extended: [1 30] mm. However, the residual error now appears much worse, but less so in the upper 75 m and above the bottom left corner where the fish is supposed to be distributed (Figure 16) and where the scattering intensity appears maximum at 18 kHz (Figure 14). The mean sizes estimated in the main part of the echogram are around 27 mm for an equivalent radius of a prolate spheroid, which according to the relationship used in the current model gives a mean length of 5 x ER = 114 mm, that might correspond to a mean swimbladder length of about 11.4 cm. Of course in the "krill" layer, the residual error is now strong (> 1) and the sizes estimated are very small as in reality the scattering is not of a gaseous type so for this type of model, the Sv measurements seem very small. More investigations must be done now, through the biological data, to check the reliability of such size results with a so rudimentary model of swimbladder.

Discussion

Frequencies considered for processing

When the 18 kHz get a stronger backscattering strength than the other frequencies, the algorithm framework, when applied with the six frequencies from 18 to 364 kHz, it classifies the samples as "gaseous sphere" with very small mean sizes (less than or around 0.1mm until 0.5mm for station MOC268), and it is accompanied in a lot of cases with high values of the residual error (above 0.5 or even larger than 1) (Figures 5, 7 and 9). Also in other situations where the classification gives a fluid-like or elastic-like model solution, the residual error does not appear so good in a lot of cases. Two questions rise from these remarks:

1. Does it make sense to look for a model fitting all the frequencies from 18 to 364 kHz, meaning that all these frequencies are able to detect the same organisms, even if it is with very variable levels? It is clear from Figure 6 that the smaller the "ka" value (i.e. $2\pi va/c$), the stronger is the domination of the gaseous part of the backscattering compared to the one coming from the fluid-like and elastic-like organisms. That is particularly the case at 18 kHz for the small sizes while at the higher frequencies the contributions of other organisms are more balanced. Therefore the 18 kHz is a strong filter for the zooplankton. The processing allows extracting only one dominating organism in the scattering process; therefore if there are gaseous organisms, the scattering produced by other ones (krill, copepods) will be hidden. If the 18 kHz is, more than the others, dominated by a gaseous scattering, the organisms contributing to the scattering at the other frequencies cannot be recognized in a processing including the 18 kHz (c.f. Figure 12b).

2. On another side, looking at the data being processed, it often appeared that when the modelisation could not fit all the six measurements, it was the point at 364 kHz that caused difficulties. With its stronger absorption, there are perhaps some situations where the signal to noise ratio for this frequency is not high enough. Or the measurements at this high frequency introduce strong constraints in the processing.

The analyses that have been done without each one of these frequencies can lead to some hypotheses on the way the results are influenced by the extreme frequencies.
The differences between the "model type" echograms of Figure 10 and of Figures 5, 7 and 9 may be explained by the strength of a gaseous type scattering, measured at 18 kHz and which dominates at some places the fluid-like or elastic-like type of scattering. By removing the 18 kHz, it becomes possible to visualise the potential presence of other types of scatterers.

On the other hand, removing the 364 kHz does not give access to the complexity of the medium, the gaseous type of scattering is still strong and the gaseous sphere model is chosen even more by the algorithm framework than when the 364 kHz is present. But there is a strong improvement in the residual errors. At least three hypotheses can be advanced to help understand this improvement. The first one is of a technical character, taking into account the higher absorption of the 364 kHz and thus a signal to noise ratio possibly insufficient for a reliable model solution. The second one is that organisms that are not so important at the lower frequencies cause a large part of the scattering at 364 kHz; therefore no common model can fit closely all the six frequencies, while it is possible without the 364 kHz. The third one is that this frequency is more decisive than the others to separate the fluid models from elastic shell model and to distinguish between the two different fluid-like models (Figure 12a). This frequency seems to introduce the highest level of constraint in the model recognition.
In the absence of both 18 and 364 kHz (Figure 13) it seems that the 38 kHz plays the 18 kHz's role when its scattering strength is higher than those of the higher frequencies, hiding the non-gaseous scatterers. On the other side without the 364 kHz the classification is simplified but the discrimination between the non-gaseous models, seems to be partly lost.

Classification results

Considering all the stations (MOCNESS and pelagic trawl) with large areas that the algorithm has categorized as small "gaseous sphere", it indicates actually a peak at 18 kHz, or at 38 kHz when there is no 18 kHz active in the processing. It can suggest the presence of gas bearing organisms, but none of the sizes estimated can match neither pearlside or fish swimbladders nor siphonophore gas inclusions. Additionally a so huge space distribution seems very unlikely. In the presence of a peak at 18 or 38 kHz, the algorithm is probably able to find a suitable solution with a small size presenting a resonance at 18 or 38 kHz, which the gaseous prolate spheroid model, being too flat, cannot provide. But with the availability of a complex fish model, as for example the fish model obtained by ray-path construction for a whole fish (Clay and Horne, 1994), that shows a maximum at a low frequency (even after the resonance), the algorithm framework might provide a more plausible categorization.

The wide categorization as “gaseous sphere” may probably be understood as a choice made due to a lack of a more accurate model for fish.

From now, only the results obtained by a processing without the 18 kHz will be commentated (Figure 10). Nevertheless there are no obvious relationships between the nets contents and the classification results. Tables 2 to 5 show that in a general manner, siphonophores, copepods, krill, Limacina and Globigerina are probably found in the whole water column at all the stations. At this stage, it can be said that for MOC266 and MOC268, the classification gives a variety of model solutions, which can represent the variety organisms that are present in the nets. For MOC260 and MOC262 a smaller number of model solutions have been extracted from the classification compared to the variety of types of organisms caught. However, the vertical distribution does not cover the whole water column, except for MOC266. Another problem is the size estimates, which presently seem far from realistic. They are too large for the organisms that the models are supposed to represent. However, copepods with an equivalent spherical radius of 0.315 mm have very low acoustic responses at the frequencies considered in this work (TS from –140 dB at 38 kHz to –103 dB at 364 kHz, from the truncated fluid sphere model). It must be reminded that D.V Holliday and C. Greenlaw have designed a high-frequency profiler precisely to detect the copepods and the other small zooplankton. So another concern that can be pointed out from these analyses, is to find a way to sample precisely what is actually detected by the echo sounders. For example, the mean sizes estimated for the targets in the “krill layer” at station PT557 (Figure 15) are perhaps the most realistic among the various results obtained.

Conclusion

This work constitutes the first real application to field data of the Multi-model multi frequency classification algorithm (Lebourges-Dhaussy & Ballé-Béganton, 2004) although other but similar approaches is also recently being developed and tested also in an operational context (c.f. Korneliussen and Ona, 2002, 2003). It is apparent however, that the multi-model classification approach has additional potential and also allows highlighting different areas in an echogram where the scattering properties of the population, and the frequency response in particular contrast each other well. What is less clear is the degree of reliability of the classification results, even in terms of the choice of the model of type of organisms, but also in quantitative terms.
This validation exercise will be extended in the near future through analyses of smaller regions of the echograms that coincide more closely the net sampling volumes. This will be followed by a more detailed analysis of species composition, abundance and size distribution for a carefully selected number ofnet tows. By this way of processing a smaller amount of acoustic data, it will be possible also to apply the DWBA models and hopefully to obtain a more quantitative insight in the comparisons by models, sizes, abundances and biovolumes. The aim of this work is to achieve a classification quality that could aid in the assessment of zooplankton abundance and to aid the separation of zooplankton from fish detections. Ultimately the inclusion of a multi-model framework approach in an operational context that could extend or improve similar approaches (c.f. Korneliussen and Ona, 2002, 2003) would be valuable in monitoring and management of marine pelagic resources.

References

Anon., 1968. Smaller mesozooplankton. Report Working Party No. 2. Pp. 153-159 *in*: Tranter, D.J. (ed.) *Zooplankton Sampling. (Monographs on oceanographic zooplankton methodology 2.)*. UNESCO, Paris. 174 pp.

Benfield M.C., Wiebe P.H., Stanton T.K., Davis C.S., Gallager S.M., Greene C.H. (1998). Estimating the spatial distribution of zooplankton biomass by combining Video Plankton Recorder and single-frequency acoustic data. Deep-Sea Research Part II 45(7): 1175-1199.

Clay, C.S. and Horne, J.K. (1994). Acoustic models of fish: the Atlantic cod (Gadus morhua). J. Acoust. Soc. Am. 96, 1661-1668.

Cochrane N.A., Sameoto D., Herman A.W., Neilson J. (1991). Multiple-frequency acoustic backscattering and zooplankton aggregations in the inner Scotian shelf basins. Can. J. Fish. Aquat. Sci. 48: 340-355.

Dalpadado, P., Ellertsen,B., Melle,W. and Skjoldal,H.R. (1998). Summer distribution patterns and biomass estimates of macrozooplankton and micronekton in the Nordic Seas. *Sarsia*, 83,103-116.

Foote, K. G., 1982. Optimizing copper spheres for precision calibration of hydroacoustic equipment. Journal of the Acoustical Society of America, 71: 742-747.

Foote, K. G., Knudsen, H. P., Vestnes, G., MacLennan, D. N., and Simmonds, E. J., 1987. Calibration of acoustic instruments for fish density estimation: A practical guide. ICES cooperative research report, 144, 69 pp.

Foote,K.G., Knudsen,H.P., Korneliussen,R.J., Nordbø,P.E. and Røang,K. (1991). Postprocessing system for echo sounder data. *J. Acoust. Soc. Am.*,90(1),37-47.

Francis, D.T.I. (1993) A gradient formulation of the Helmholtz integral equation for acoustic radiation and scattering. *J. Acoust. Soc. Am.*,93,1700-1709.

Francis, D.T.I., Foote,K.G., Knutsen,T. and Calise,L. (1999) Modeling the target strength of *Calanus finmarchicus*. *Acta Acoustica*, 85,S124 & *J. acoust. Soc. Am.*,105,1050.

Gajate, J., Ponce, R., Peña, M.A., Iglesias, M. and P.G. Fernandes (2004). SIMFAMI database: An application of the Spanish software SIRENO. ICES CM2004/R:27.

Greenlaw, C.F. (1977). Backscattering spectra of preserved zooplankton. J. Acoust. Soc. Am. 62:44-52.

Greenlaw, C.F. (1979). Acoustical estimation of zooplankton populations. Limnol. Oceanogr. 24:226-242.

Greenlaw, C.F. and Johnson, R.K. (1983). Multiple-frequency acoustical estimation. Biological Oceanography 2 (2-3-4):227-252

Halliday, N.C. (2001) A comparison of morphometric and geometric methods for the estimation of individual zooplankton volumes. Sarsia, 86:101-105.

Halliday,N.C., S.H. Coombs and C. Smith (2001) A comparison of LHPR and OPC data from vertical distribution sampling in a Norwegian fjord. Sarsia()?, 86:87-99.

Harris, R.P., H.R. Skjoldal, Lenz,J. and Wiebe,P. and M. Huntley, 2000. ICES Zooplankton Methodology Manual. ISBN 0-12-327645-4.

Herman, A.W., 1988. Simultaneous measurement of zooplankton and light attenuance with a new optical plankton counter. *Continental Shelf Research*, Vol. 8, No. 2, pp. 205-221, 1988.

Herman, AW. 1992. Design and calibration of a new optical plankton counter capable of sizing small zooplankton. *Deep-Sea Research*,39, 3-4A, 395-415.

Herman, A.W, Cochrane, NA; Sameoto, DD. 1993. Detection and abundance estimation of euphausiids using an optical plankton counter. *Mar. Ecol. Prog. Ser*.,94,2,165-173.

Hirche,H-J., Hagen,W., Mumm,N. and Richter, C. (1994) The Northeast Water Polynya, Greenland Sea III. Meso- and macrozooplankton distribution and production of dominant herbivorous copepods during spring. *Polar Biol*.,14:491-503

Holliday, D.V. (1992). Zooplankton acoustics. Oceanography of the Indian Ocean. B.N. Desai (Ed.):733-740

Holliday D.V., Pieper R.E. (1980). Volume scattering strengths and zooplankton distributions at acoustic frequencies between 0,5 and 3 MHz. J. Acoust. Soc. Am. 67(1): 135-146.

Johnson, R.K. (1977). Sound scattering from a fluid sphere revisited. J. Acoust. Soc. Am. 61(2): 375-377.

Kaartvedt,S., Melle,W., Knutsen,T. and Skjoldal,H.R.S. (1996) Vertical distribution of fish and krill beneath water of varying optical properties. *Mar. Ecol. Progr. Ser*.,136,51-58.

Knutsen, T. (in prep.) Converting BI500/BEI files to the HydroAcoustic Common format (HAC) - a BEI/BI500 to HAC converter running in a unix environment.

Korneliussen, R. J., Diner, N., Ona, E., Fernandes, P. G. (2004). Recommendations for the collection of multi-frequency acoustic data. ICES CM2004/R :36, 15pp.

Korneliussen, R. J., and Ona, E. (2002). An operational system for processing and visualising multi-frequency acoustic data. ICES Journal of Marine Science, 59: 293-313.

Korneliussen, R. J., and Ona, E. (2003). Synthetic echograms generated from the relative frequency response. ICES Journal of Marine Science, 60, 636 - 640.

Korneliussen, R. J. (2004). The Bergen Echo Integrator post-processing system, with focus on recent improvements. Fisheries Research 68 (2994) 159-169.

Korneliussen, R. (2000). Measurement and removal of echo integration noise. ICES Journal of Marine Science, 57: 1204-1217.

Kristensen A., Dalen J. (1986). Acoustic estimation of size distribution and abundance of zooplancton. J. Acoust. Soc. Am. 80(2): 601-611.

Lawson C.L. and R.J. Hanson. 1974. Solving least squares problems. Prentice Hall, New Jersey. 340 pp.

Lebourges-Dhaussy A. (1996). Caractérisation des populations planctoniques par acoustiques multifréquence. Océanis 22(1): 71-92.

Lebourges-Dhaussy A. and Ballé-Béganton J. (2004). Multifrequency multimodel zooplankton classification. ICES CM 2004/R:22.

Melle,W., Kaartvedt,S.,Knutsen,T., Dalpadado,P. and Skjoldal,H.R. (1993). Acoustic visualization of large scale macroplankton and micronekton distributions across the Norwegian shelf and slope of the Norwegian Sea. *ICES Council meeting*, L:44:1-25.

Melle,W., (1998) Reproduction, life cycles, and distributions of *Calanus finmarchicus*, *C. glacialis*, and *C. hyperboreus* in relation to environmental conditions in the Barents Sea. Dr. scient. thesis, ISBN 82-7744-046-4, University of Bergen.

Pieper, R.E. and D.V. Holliday (1984). Acoustic measurements of zooplankton distributions in the sea. J. Cons. Int. Expl. Mer, 41: 226-238.

Sameoto D., Cochrane N., Herman A. (1993). Convergence of acoustic, optical, and net-catch estimates of euphausiid abundance : use of artificial light to reduce net avoidance. Can. J. Fish. Aquat. Sci. 50: 334-346

Simard, Y., I. McQuinn, N. Diner, and C. Marchalot. 1999. The world according to ***HAC***: summary of this hydroacoustic standard data format and examples of its application under diverse configurations with various echosounders and data acquisition software. ICES-Fisheries Acoustics Sciences and Technology meeting, St. John's, Newfoundland, Canada, 20-22 April 1999, Working paper. 14 pp.

Simard, Y., I. McQuinn, M. Montminy, C. Lang, D. Miller, C. Stevens, D. Wiggins and C. Marchalot. 1997. Description of the ***HAC*** standard format for raw and edited hydroacoustic data, version 1.0. Can. Tech. Rep. Fish. Aquat. Sci. 2174: vii + 65 pp.

Siegel, V. 2000a. Krill (Euphausiacea) life history and aspects of population dynamics. *Can. J. Fish Aquat. Sci.* 57: 130-150.

Siegel, V. 2000b. Krill (Euphausiacea) demography and variability in abundance and distribution. *Can. J. Fish Aquat. Sci.* 57: 130-150.

Simard,Y., de Ladurantaye,R. Therriault,J.-C. (1986). Aggregation of euphausiids along a coastal shelf in an upwelling environment. *Mar. Ecol. Prog. Ser*.,32(2-3),203-215.

Simard,Y. and Mackas,D.L. (1989). Mesoscale aggregations of euphausiid sound scattering layers on the continental shelf of Vancouver Island. *Can. J. Fish. Aquat. Sci*.,46(7),1238-1247.

Stanton, T.K. (1989). Simple approximate formulas for backscattering of sound by spherical and elongated objects. J. Acoust. Soc. Am. 86 (4):1499-1510.

Stanton, T.K. (1990). Sound scattering by zooplankton. Rapp. P.-v. Réun. Conseil int. Explor. Mer 189: 353-362.

Stanton, T.K., P.H. Wiebe, D. Chu, M.C. Benfield, L. Scanlon, L. Martin and R.L. Eastwood (1994). On acoustic estimates of zooplankton biomass. ICES Journal of Marine Science 51(4): 505-512.

Stanton, T.K. and D. Chu, (2000). Review and recommendations for the modeling of acoustic scattering by fluid-like elongated zooplankton: euphausiids and copepods. ICES Journal of Marine Science, 57: 793-807.

Torgersen,T., Kaartvedt,S., Melle,W. and Knutsen,T. (1997). Large scale distribution of acoustical scattering layers at the Norwegian Sea continental shelf and the eastern Norwegian Sea. *Sarsia*,82,87-96.

Valdemarsen,J.W. and Misund,O.A. (1995). Trawl designs and techniques used by Norwegian Research Vessels to sample fish in the pelagic zone. Pp. 135-144 in Hylen,A (ed) : Precision and relevance of pre-recruit studies for fishery management related to fish stocks in the Barents Sea and adjacent. Proceedings of the sixth IMR-PINRO Symposium, Bergen, 14-17 June 1994.

Weill, A., Scalabrin, C., Diner, N. (1993). MOBIES-B: an acoustic detection description software. Application to shoal species classification. Aquatic living resources 6(3): 255-267.

Wiborg, K.F. (1954). Investigations on zooplankton in coastal and offshore waters of western and north-western Norway with special reference to the copepods. *Fisk.Dir.Skr.Ser.HavUnders*. 11(1):1-246.

Wiebe, P.H., Burt, K.H., Boyd, S.H., and Morton, A.W. 1976. A multiple opening/closing net and environmental sensing system for sampling zooplankton. *J. Mar. Res.*, 34,313-326.

Wiebe, P.H., Morton A.W., Bradley, A.M., Backus R.H., Craddock J.E., Barber V., Cowles T.J. & G.R. Flierl, 1985. New developments in the MOCNESS, an apparatus for sampling zooplankton and mikronekton. *Marine Biology*,87,313-323.

Wiebe,P.H., H.R. Skjoldal, L. Postel, M.D. Allison, R.C. Growman and T. Knutsen (2002) ICES/GLOBEC Sea-Going Zooplankton Workshop for intercalibration of Plankton Samplers. A compilation of data, metadata, and visual material. ICES Cooperative Research Report NO. 250:1-22 plus 4 CD's.

Wiebe, P.H. and M.C. Benfield (2003) From the Hensen Net towards four-dimensional biological oceanography. Progress in Oceanography, 56(1): 7-136.

Østvedt, O.J. (1955). Zooplankton investigations from weather ship M in the Norwegian Sea, 1948-1949. *Hvalråd.Skr*.40:1-93.

Table 1. Settings used in the models for the data processings, including density (“g”) and sound speed (“h”) contrasts between the organisms and their surrounding medium.

		Shape, material	Incident angle	Std deviation of angles	g	h	L/a	L/b	ψ	ρ/L	Reflection coefficient r
Copepods	TFS (Holliday 1992)	fluid sphere			1.12	1.09					
	DWBA (Stanton, Chu 2000)	fluid ellipsoid	0	30	1.02	1.06	2.55	L/a	π/2		
	High-pass (Stanton, 89)	fluid sphere			1.043	1.05					
	High-pass (Stanton, 89)	fluid prolate spheroid			1.043	1.05	5				
Small euphausiids (L<15mm)	DWBA (Stanton, Chu 2000)	fluid cylinder	20	20	1.016	1.02	10.5			3	
Large euphausiids (L>15mm)	DWBA (Stanton, Chu 2000)	fluid cylinder	20	20	1.018	1.02	13			3	
Euphausiids	High-pass (Stanton, 89)	fluid bent cylinder			1.043	1.05	10.5			0.5	
Gastropods	High-pass elastic shelled (Stanton & al 1994)	elastic sphere									0.5
“Swimbladder”	High-pass (Stanton, 89)	gaseous prolate spheroid			0.0012	0.22	5				
Gas bubble	DWBA (Stanton& al 1998)	gaseous sphere	0	30	0.0024	0.22	2				
	High-pass (Stanton, 89)	gaseous sphere			0.0012	0.22					

Table 2. Composition of the MOC260 catches.

Plankton/ Trawl station	**Depth (m)**	**Qualitative assessment >180 µm**	**>1000 µm and < 2000 µm**	**Qualitative assessment >2000 µm**
MOCNESS 260 **Oct. 24th 02:00-02:22**	180-120	Small calanoid copepods, small Concoecia, Limacina, Globigerina	Some krill juveniles and/or krill larvae	Fish larvae(N=1,L=10mm), Shrimp (N=1,L=16mm), Siphonophore remains, Krill(N=33, L=~10-20mm)
	120-80	Small calanoid copepods, small Concoecia, Limacina, Globigerina	Some krill juveniles and/or krill larvae, some calanoid copepods	Some siphonophore remains, Krill(N=18, L=~10-20mm)
	80-50	Mainly small calanoid copepods	Some small krill, siphonophore remains	Many siphonophore swimming bells (nectophores) and remains Pearlside (N=5, 11-22 mm) Krill (N=7, ~11-19 mm)
	50-25	Mainly small calanoid copepods and Limacina	Some small krill and calanoid copepods	A few remains of siphonophores Pearlside (N=2, 22-23 mm) Krill_Mn (N=2, ~15 mm) Krill_Nc (N=32, ~13 mm)
	25-0m	Mainly calanoid copepods and Limacina	Some small krill and calanoid copepods	Many siphonophore swimming bells Krill_Mn (N=5, ~16 mm) Krill_indet (N=10, ~12 mm)

Krill_Mn = *Meganyctiphanes norvegica*
Krill_Nc = *Nyctiphanes couchi*
Krill_Sl =*Stylocheiron longicorne*
Krill_Nm =*Nematoscelis megalops*
Krill_Ek =*Euphausia krohnii*
Krill_Ti = *Thysanoessa inermis*
Krill_Tl =*Thysanoess longicaudata*

Table 3. Composition of the MOC262 catches.

Plankton/ Trawl station	Depth (m)	Qualitative assessment >180 µm	Qualitative assessment >1000 and < 2000 µm	Qualitative assessment >2000 µm
MOCNESS 262 Oct. 24th 16:53-17:08	263-200	Small calanoid copepods, Chaetognaths, a few Limacina	Chaetognaths, calanoid copepods, krill juveniles and/or krill larvae	Chaetognaths, Krill_Mn (N=11,L=27mm) Krill_Nm(N=8,L=13.6mm) Krill_Sl (N=1,L=17mm)
	200-150	Mainly small calanoid copepods	Calanoid copepods, krill juveniles and/or krill larvae	Calanoid copepods, Krill_Mn (N=25,L=19.8mm) Krill_Nm(N=4,L=21mm) Krill_Nc(N=1,L=10mm) Krill_Ti (N=2,L=11.5mm)
	150-100	Mainly small calanoid copepods, Globigerina,	Calanoid copepods, Siphonophore remains, krill juveniles and/or krill larvae	Siphonophore remains, Krill_Mn (N=15,L=19.4mm) Krill_Nm(N=9,L=19.2mm) Krill_Sl (N=1,L=8mm) Krill_Ti (N=11,L=11.7mm) Krill_Nc(N=1,L=10mm)
	100-50	Mainly small calanoid copepods, Globigerina, Concoecia	Calanoid copepods, Siphonophore remains, krill juveniles and/or krill larvae	Siphonophore remains, Krill_Mn (N=5,L=17.8mm) Krill_Nm(N=1,L=21mm) Krill_Ek (N=4,L=14.5mm) Krill_Ti (N=3,L=10.3mm) Pearlside (N=3,L=17.7mm)
	50-25	Mainly small calanoid copepods, Gobigerina and a few Limacina	Calanoid copepods, some krill juveniles and/or krill larvae	Siphonophore remains, Krill_Nc(N=7,L=8.6mm) Krill_Ti (N=7,L=10.1mm) Pearlside (N=2,L=15mm)
	25-0m	Mainly small calanoid copepods and a few Limacina	Calanoid copepods, some krill juveniles and/or krill larvae	Krill_Mn(N=2,L=19.5mm) Krill_Nc(N=1,L=13mm) Krill_Ti (N=2,L=12.5mm) Pearlside (N=5,L=13.2mm)

Krill_Mn = Meganyctiphanes norvegica
Krill_Nc = Nyctiphanes couchi
Krill_Sl =Stylocheiron longicorne
Krill_Nm =Nematoscelis megalops
Krill_Ek =Euphausia krohnii
Krill_Ti = Thysanoessa inermis
Krill_Tl =Thysanoess longicaudata

Table 4. Composition of the MOC266 catches.

Plankton/ Trawl station	Depth (m)	Qualitative assessment >180 µm	Qualitative assessment >1000 and < 2000 µm	Qualitative assessment >2000 µm
MOCNESS 266 Oct. 25th 11:40-11:55	220-200	Small calanoid copepods, a few Limacina	Chaetognaths, calanoid copepods, krill juveniles and/or krill larvae	Chaetognaths, Aglanta, Siphonophore remains, Krill_Mn (N=7,L=21mm) Krill_Ek (N=4,L=15mm) Krill_Nm (N=1,L=22mm) Krill_Sl (N=1,L=9mm)
	200-150	Mainly small calanoid copepods, a few Limacina	Chaetognaths, calanoid copepods, krill juveniles and/or krill larvae, siphonophore remains	Large amount of siphonophore swimming bells (nectophores) and remains
	150-100	Mainly small calanoid copepods, a few Limacina and Concoecia, Globigerina, siphonophore remains	Siphonophore remains, calanoid copepods	Siphonophore swimming bells (nectophores) and remains
	100-50	Mainly small calanoid copepods and Limacina	Some Calanus, some amphipods	Siphonophore remains
	50-25	Mainly calanoid copepods and a few Limacina	Some calanoid copepods, some krill juveniles and/or krill larvae	Many siphonophores swimming bells
	25-0 m	Mainly small calanoid copepods and a few Limacina	calanoid copepods and some siphonophore remains	Large amount of siphonophore swimming bells, some calanoid copepods,

Krill_Mn = *Meganyctiphanes norvegica*
Krill_Nc = *Nyctiphanes couchi*
Krill_Sl =*Stylocheiron longicorne*
Krill_Nm =*Nematoscelis megalops*
Krill_Ek =*Euphausia krohnii*
Krill_Ti = *Thysanoessa inermis*
Krill_Tl =*Thysanoess longicaudata*

Table 5. Composition of the MOC268 catches.

Plankton/ Trawl station	**Depth (m)**	**Qualitative assessment >180 µm**	**Qualitative assessment >1000 and < 2000 µm**	**Qualitative assessment >2000 µm**
MOCNESS 268 Oct. 25th 20:10-20:20	110-80	Small calanoid copepods, a few Limacina	Calanoid copepods, krill juveniles and/or krill larvae, Siphonophore remains	Shrimp_indet (N=3; 40,23,15mm), siphonophore remains, Mysidae, Gammaridae
	80-50	Mainly small calanoid copepods, a few Limacina and Globigerina	Calanoid copepods, krill juveniles and/or krill larvae, siphonophore remains	Chaetognaths, siphonophore remains
	50-0m	Mainly small calanoid copepods, a few Limacina and Globigerina	Calanoid copepods, siphonophore remains, krill juveniles and/or krill larvae	Siphonophore remains, krill juveniles and/or krill larvae

Echogram at 200 kHz	at 364 kHz

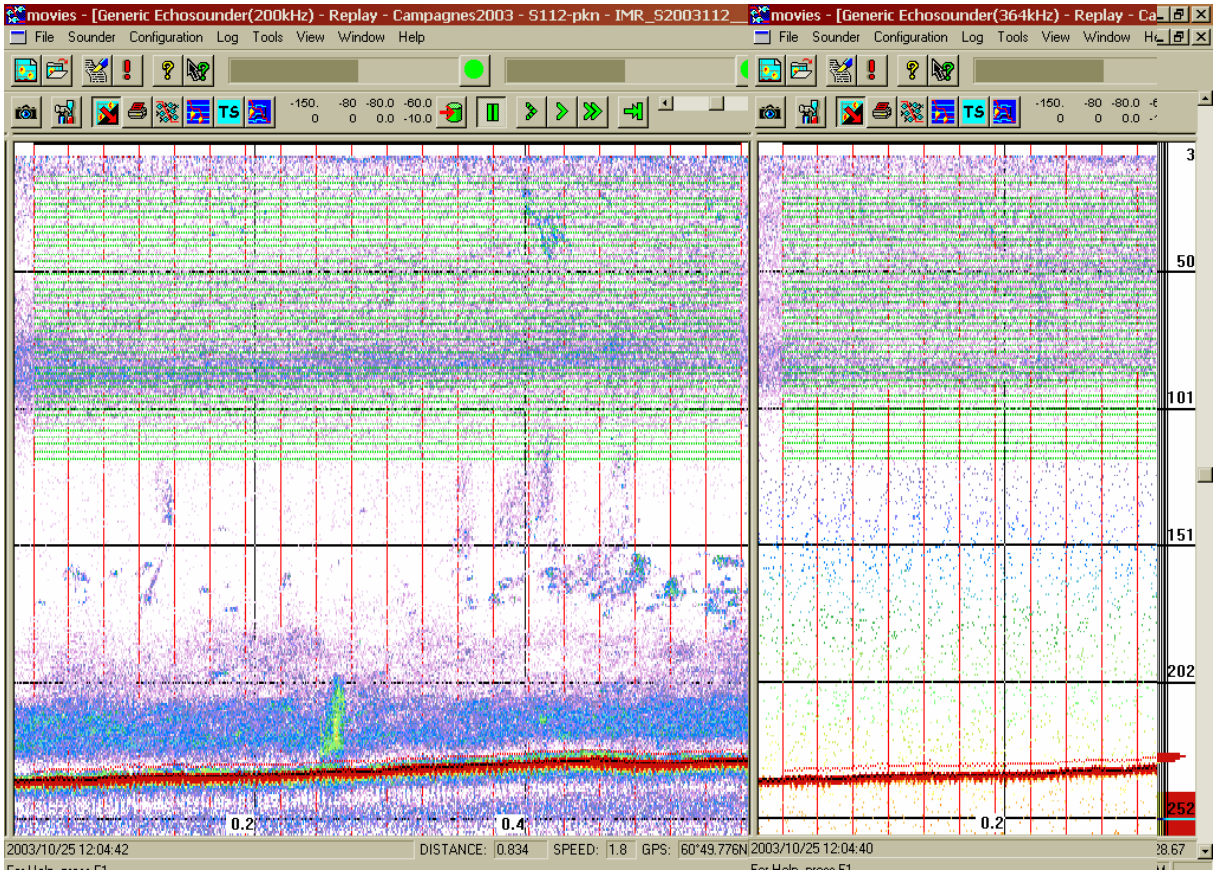

Figure 1. Integration cells (green lines) for the Mocness' station 266 shown on the echogram at 200 kHz (left) and on a part of the echogram at 364 kHz (right) to show the absorption at this high frequency. Twenty ESUs processed as as many of vertical profiles. Layers are of 2.60 meters high from 15 meters to 119 meters deep.

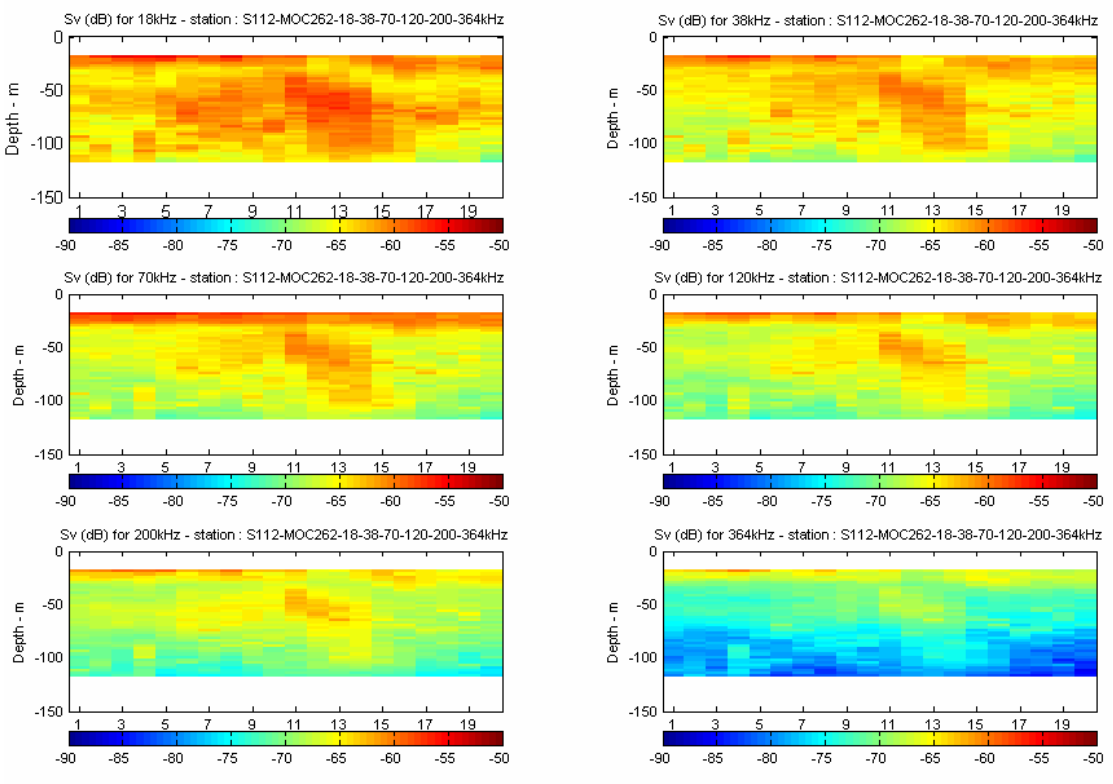

Figure 2. Station MOCNESS 262: The S_vs for the six frequencies with a decrease from the low to the high frequencies.

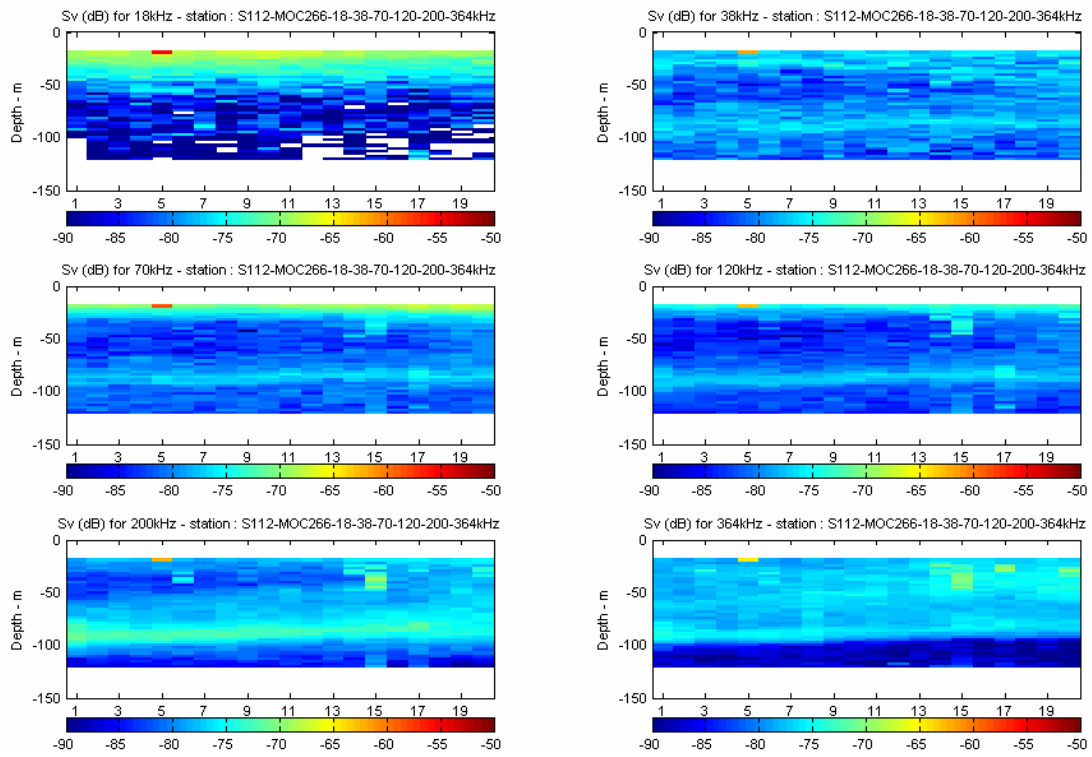

Figure 3. Station MOCNESS 266: The S_vs for the six frequencies with various trends versus frequency, according to the parts of the echogram.

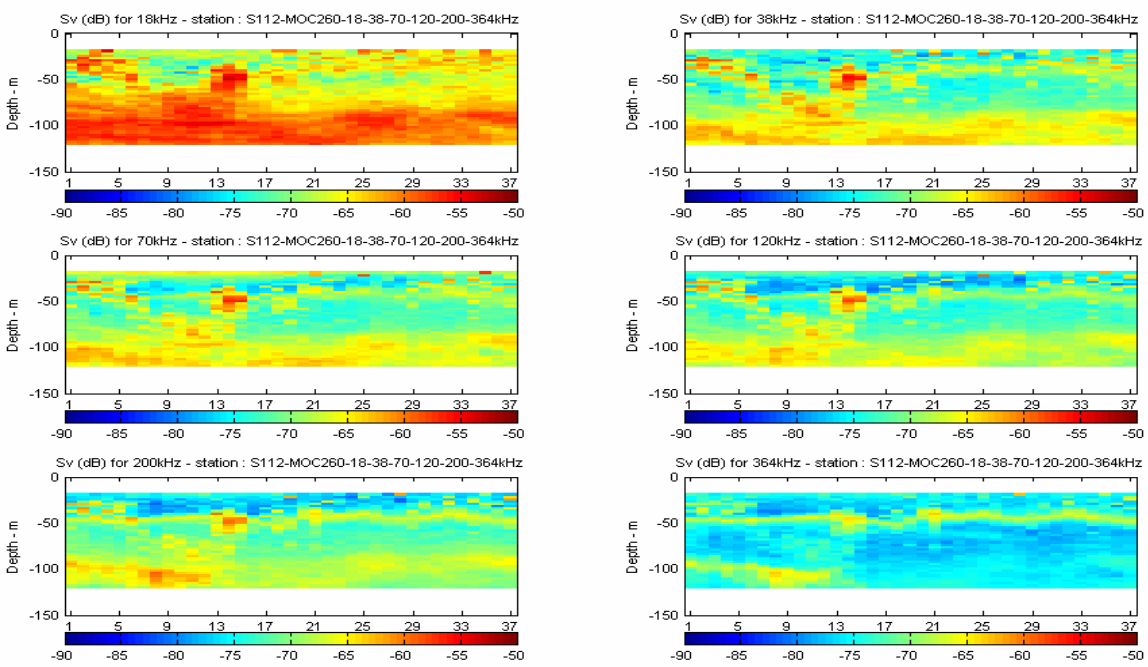

(a)

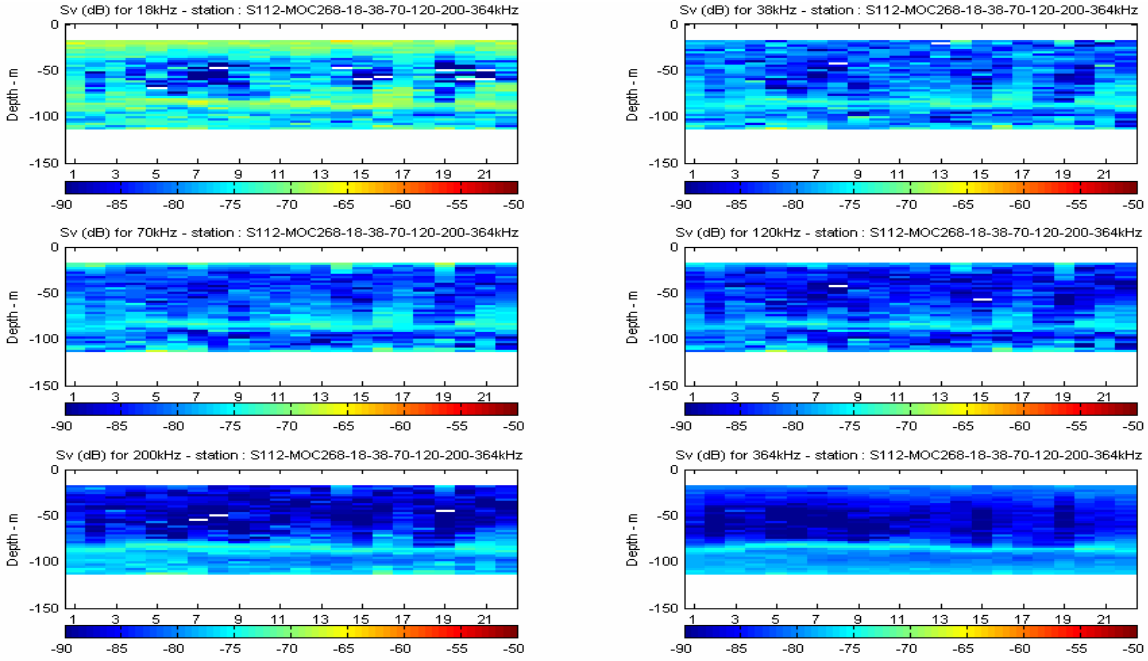

(b)

Figure 4. Stations MOCNESS 260 (a), 268 (b): The S_vs for the six frequencies.

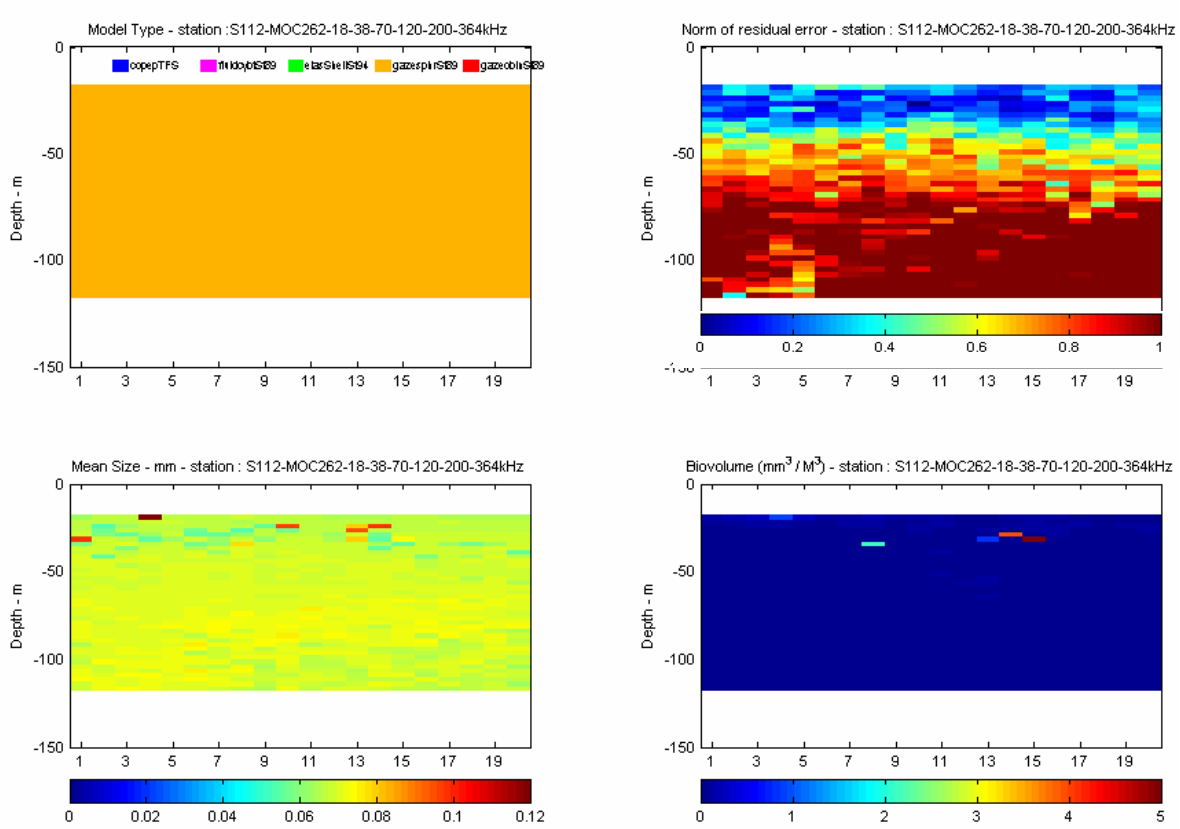

Figure 5. Results obtained from the classification algorithm on the MOC262's station: Top left: model extracted, here pure gaseous sphere fitting the Stanton 89's high pass model

Top right: Norm of the corresponding residual error for each integration cell; the lowest is the best. Above 1, the fit is bad. Below 75m there is a bad fit for a large part of the echogram.
Bottom left: Weighted average size (mm) of the extracted population in each integration cell.
Bottom right: Corresponding biovolume (mm^3/m^3).

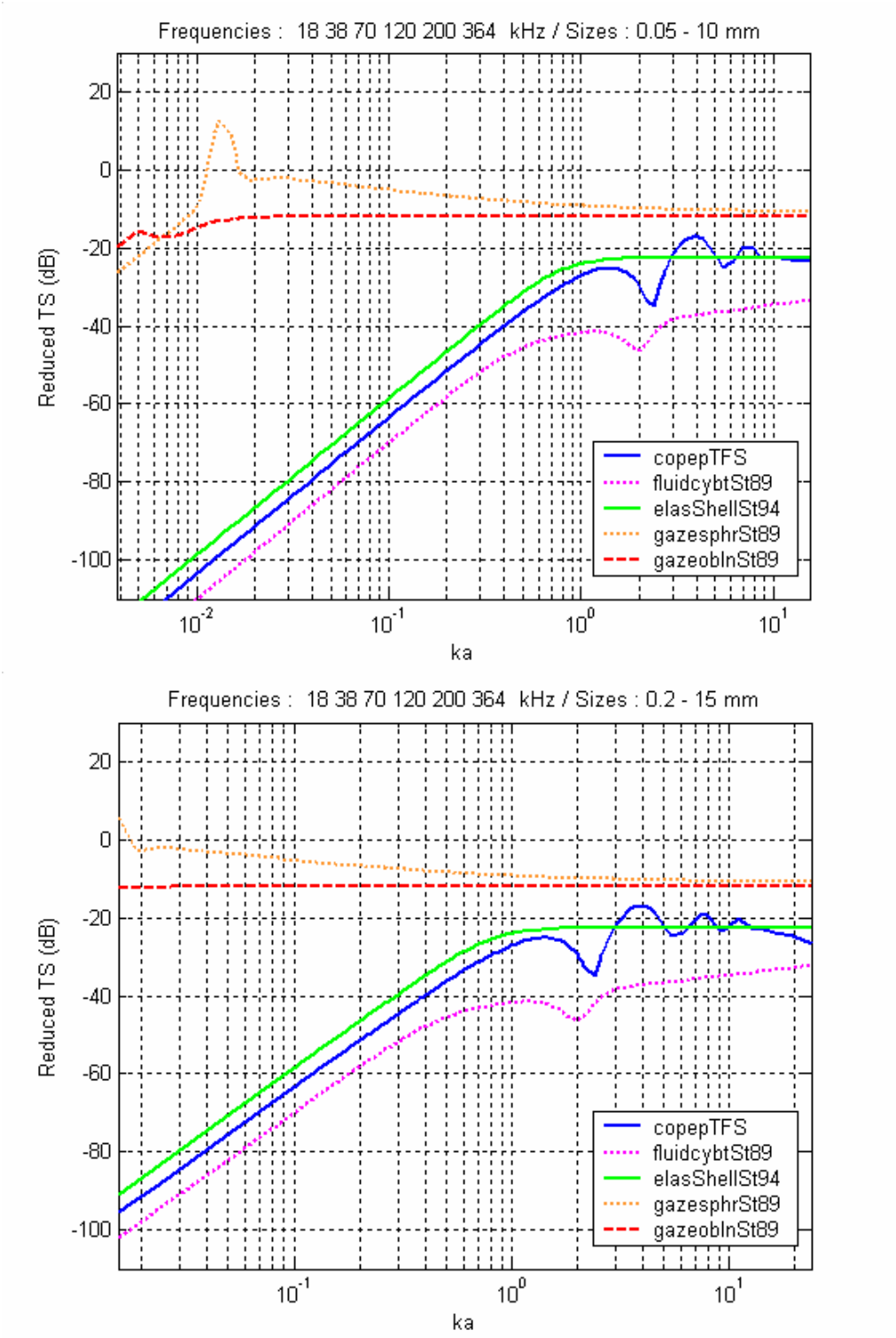

Figure 6: Reduced Target Strength versus ka, for frequencies from 18 to 364 kHz and equivalent radius from 0.05 to 15 mm.
The reduced target strength is $10\log(\sigma_{bs}/\pi a^2)$ for a sphere and $10\log(\sigma_{bs}/L^2)$ for the other shapes. For the fluid bent cylinder L has been taken equal to 10.5*a (Stanton 89); for the gaseous prolate spheroid, L has been taken equal to 5*a.

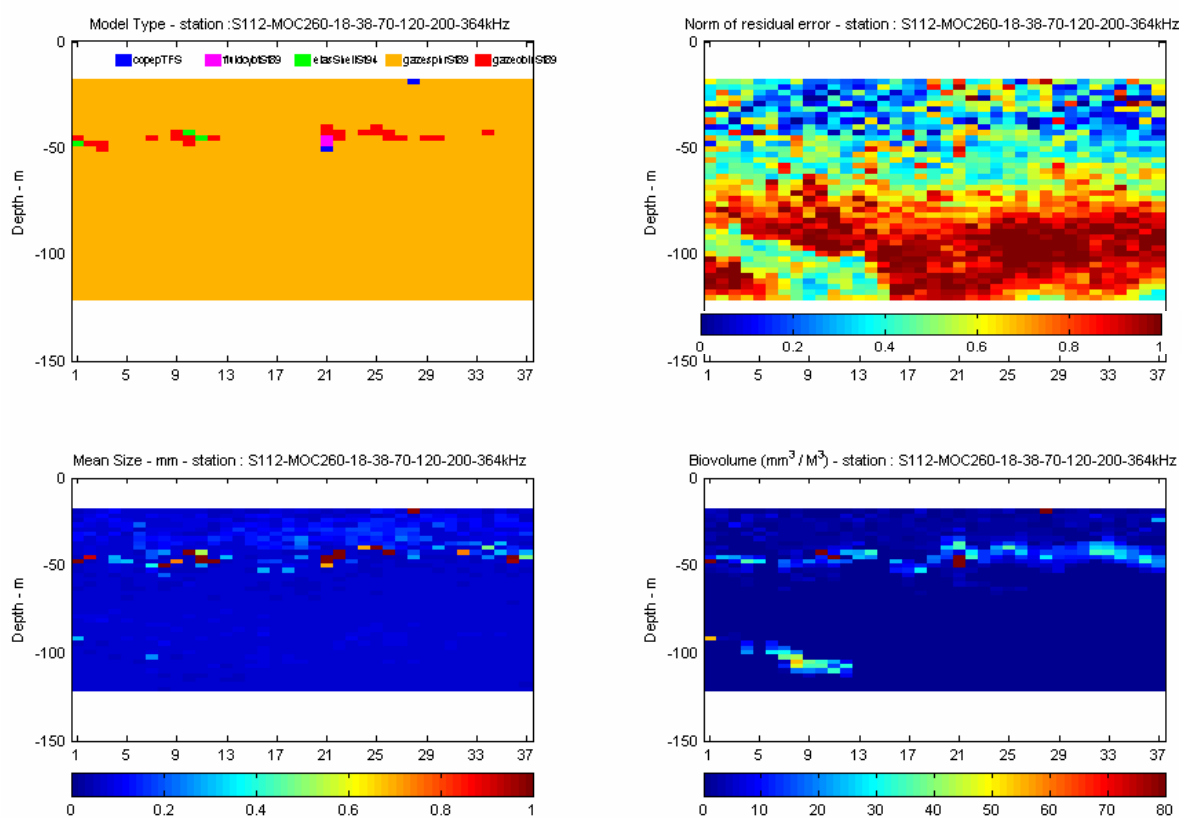

Figure 7. Results obtained from the classification algorithm for the MOC260's station:
Top left: model extracted, here pure gaseous sphere fitting the Stanton 89's high pass model

Top right: Norm of the corresponding residual error for each integration cell; the lowest is the best. Above 1, the fit is bad. Below 75m there is a bad fit for a large part of the echogram.
Bottom left: Weighted average size (mm) of the extracted population in each integration cell.
Bottom right: Corresponding biovolume (mm^3/m^3).

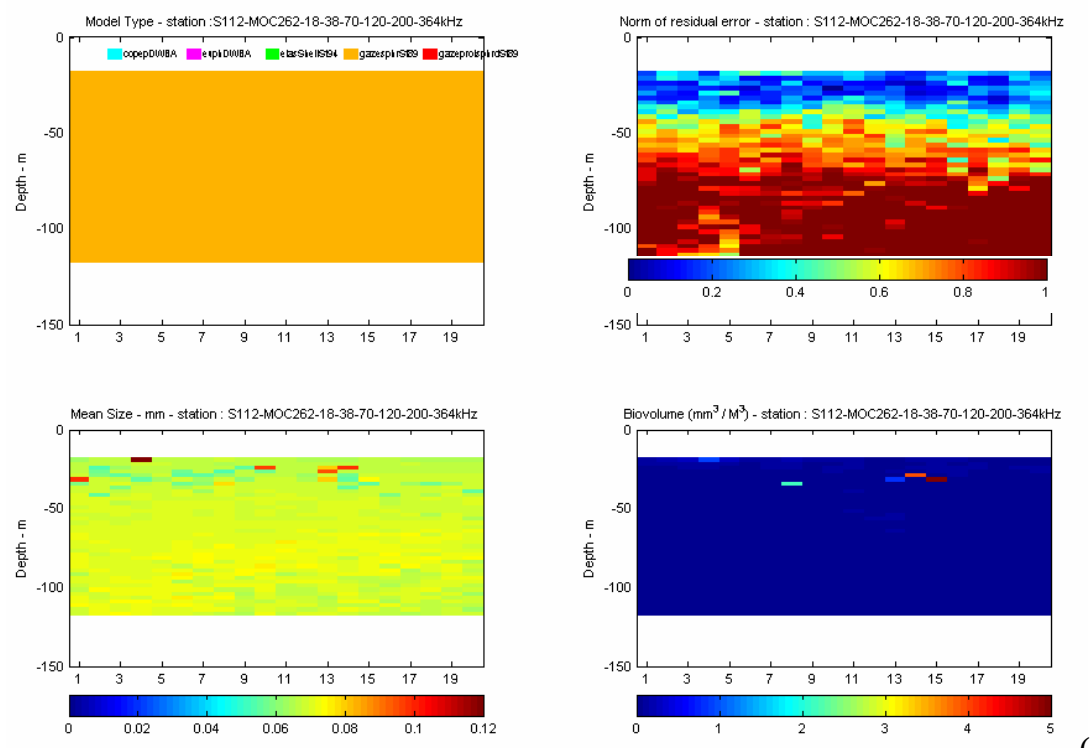

(a)

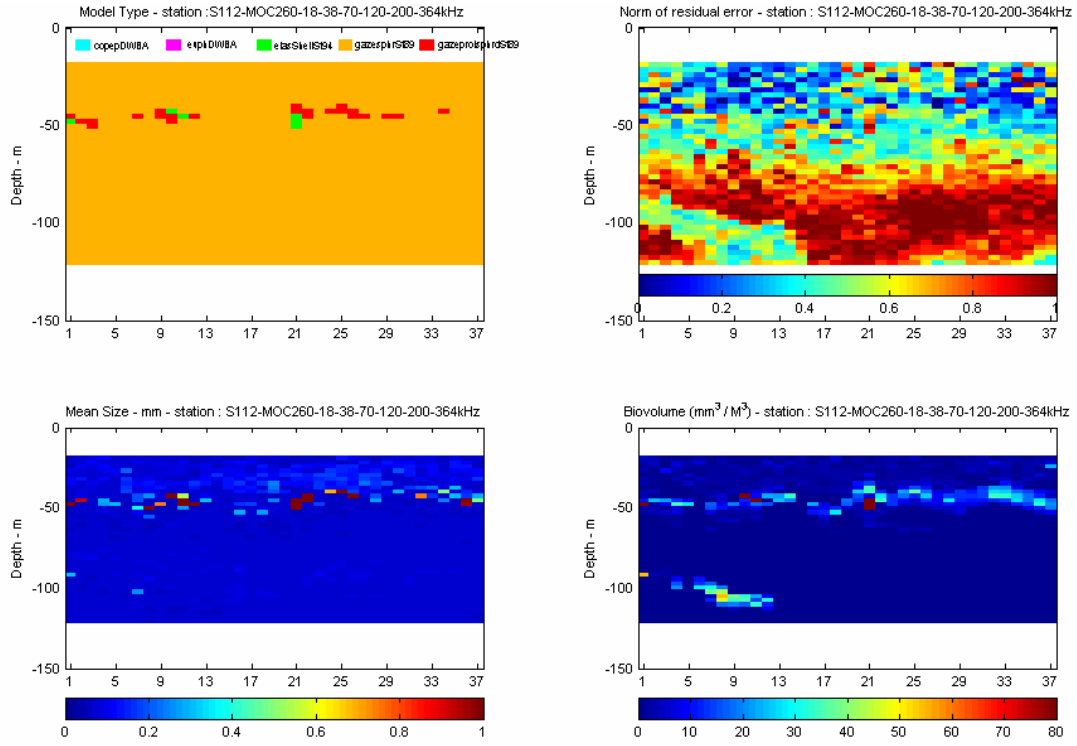

(b)

Figure 8. Results of the classification processing on stations MOC 262 and 260, with the DWBA models for copepods (fluid ellipsoid) and euphausiids (fluid bent cylinder, two g and h values for small and large euphausiids).

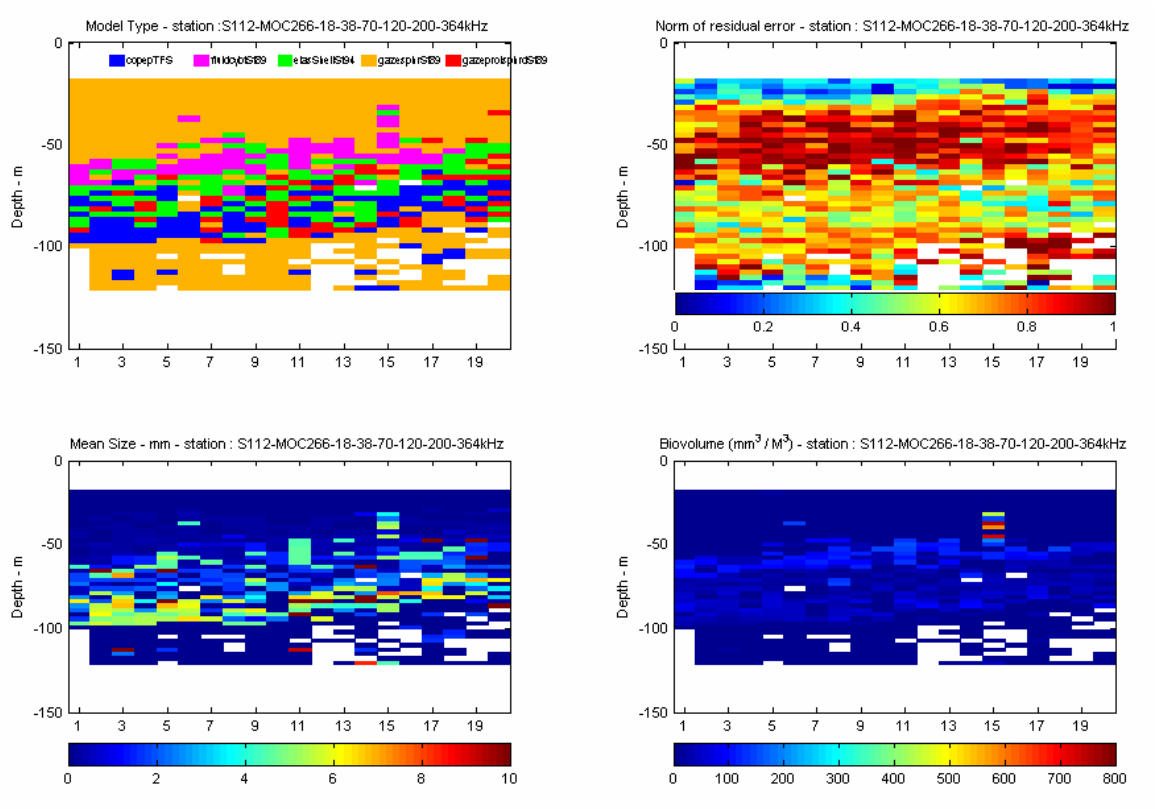

(a)

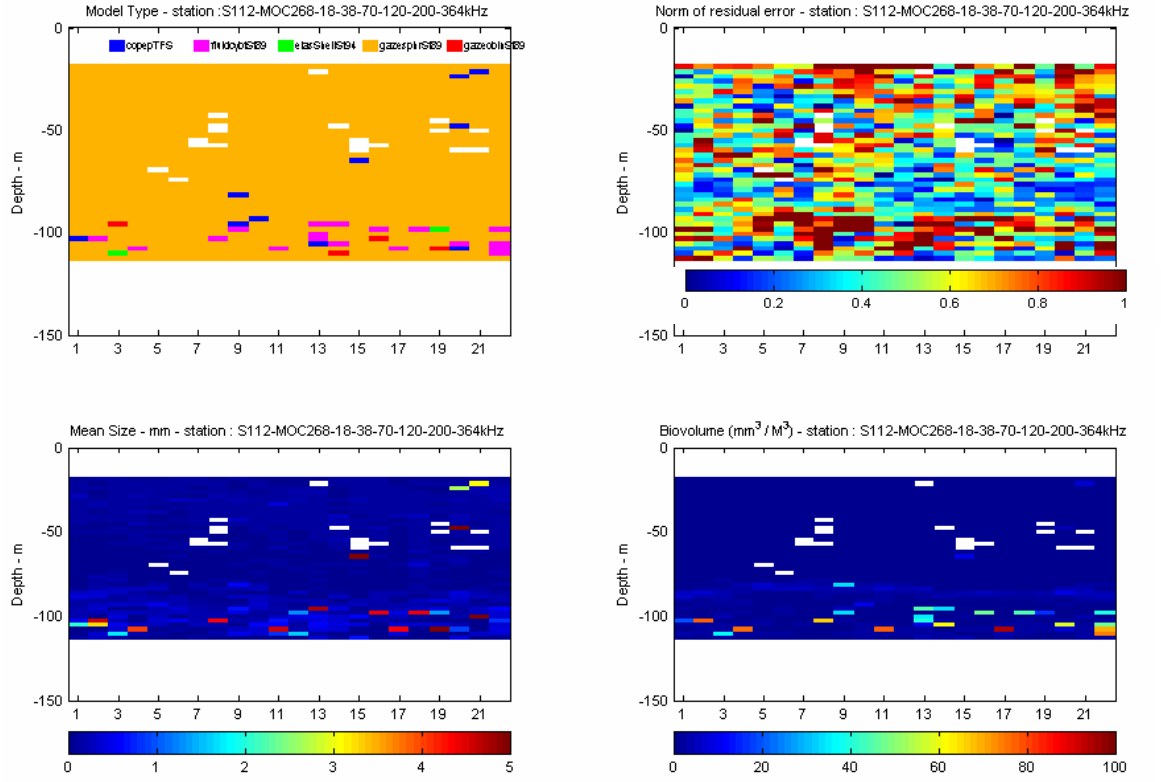

(b)

Figure 9. Results of the MOC266 (a) and 268 (b) stations processing. Legend for the models:

TruncFldSph HPFlBentCyl HPElasShell HPGasSphere HPGasProlSphd

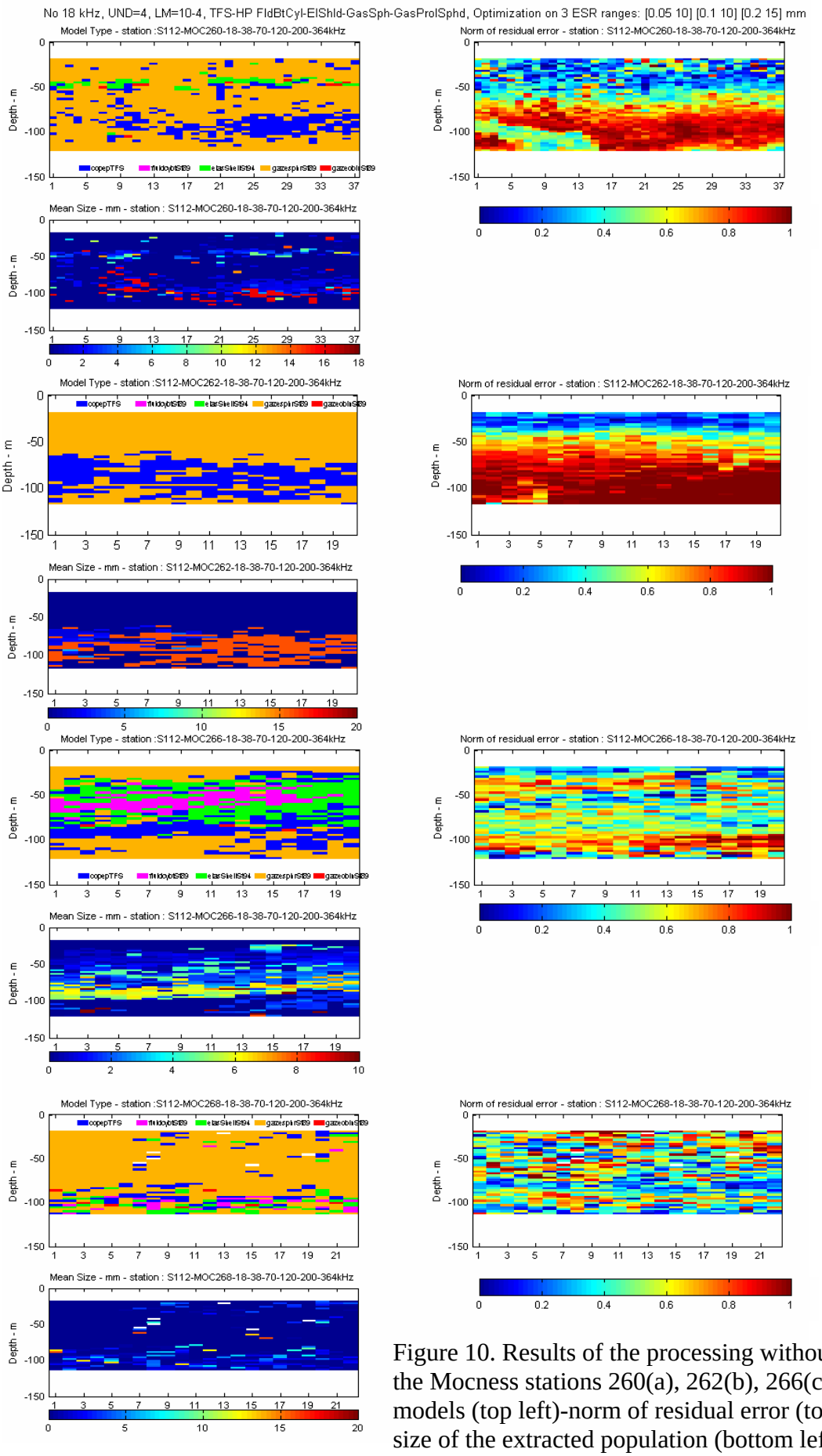

Figure 10. Results of the processing without 18 kHz for the Mocness stations 260(a), 262(b), 266(c) and 268(d): models (top left)-norm of residual error (top right)-mean size of the extracted population (bottom left).

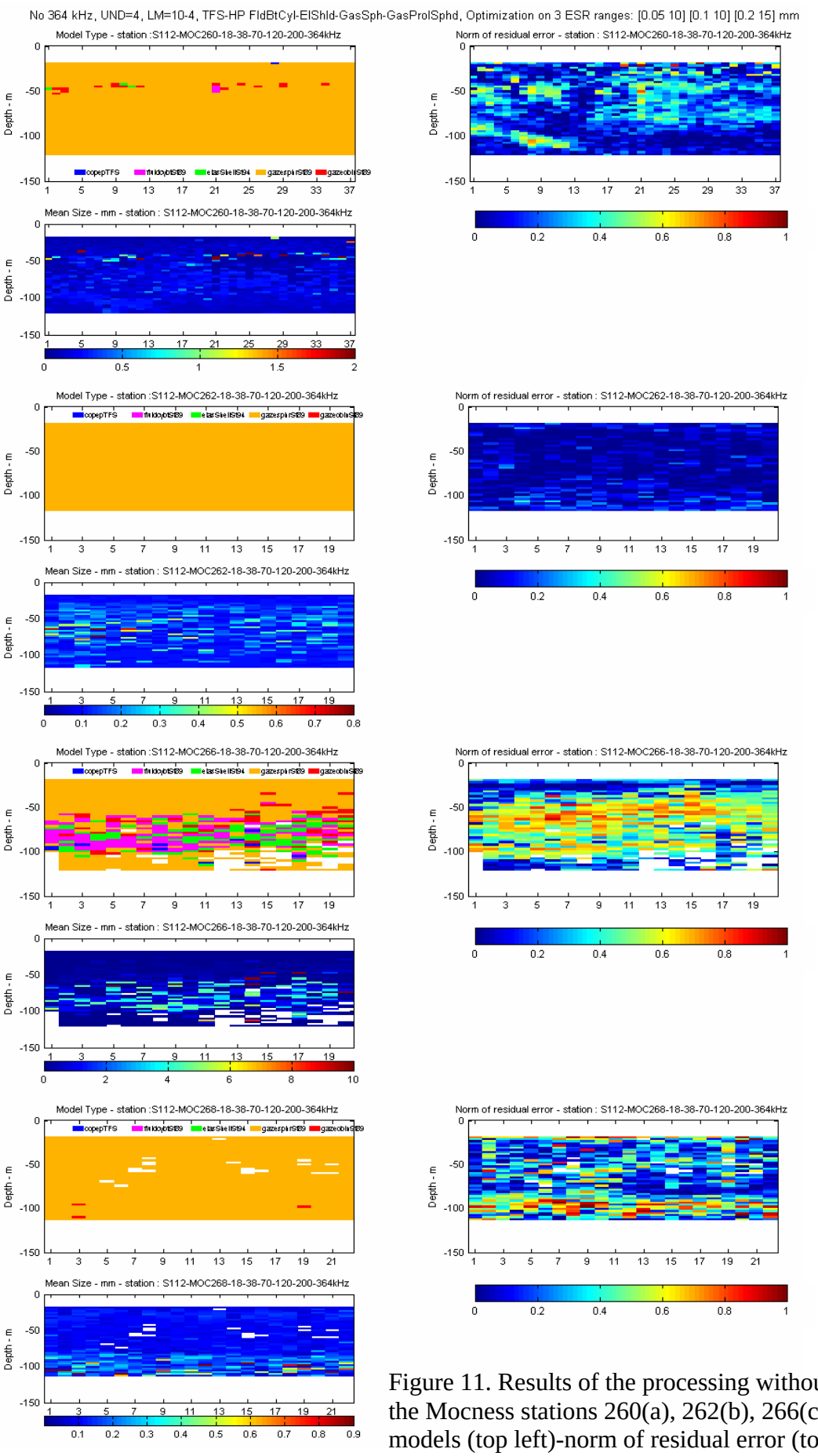

Figure 11. Results of the processing without 364 kHz for the Mocness stations 260(a), 262(b), 266(c) and 268(d): models (top left)-norm of residual error (top right)-mean size of the extracted population (bottom left).

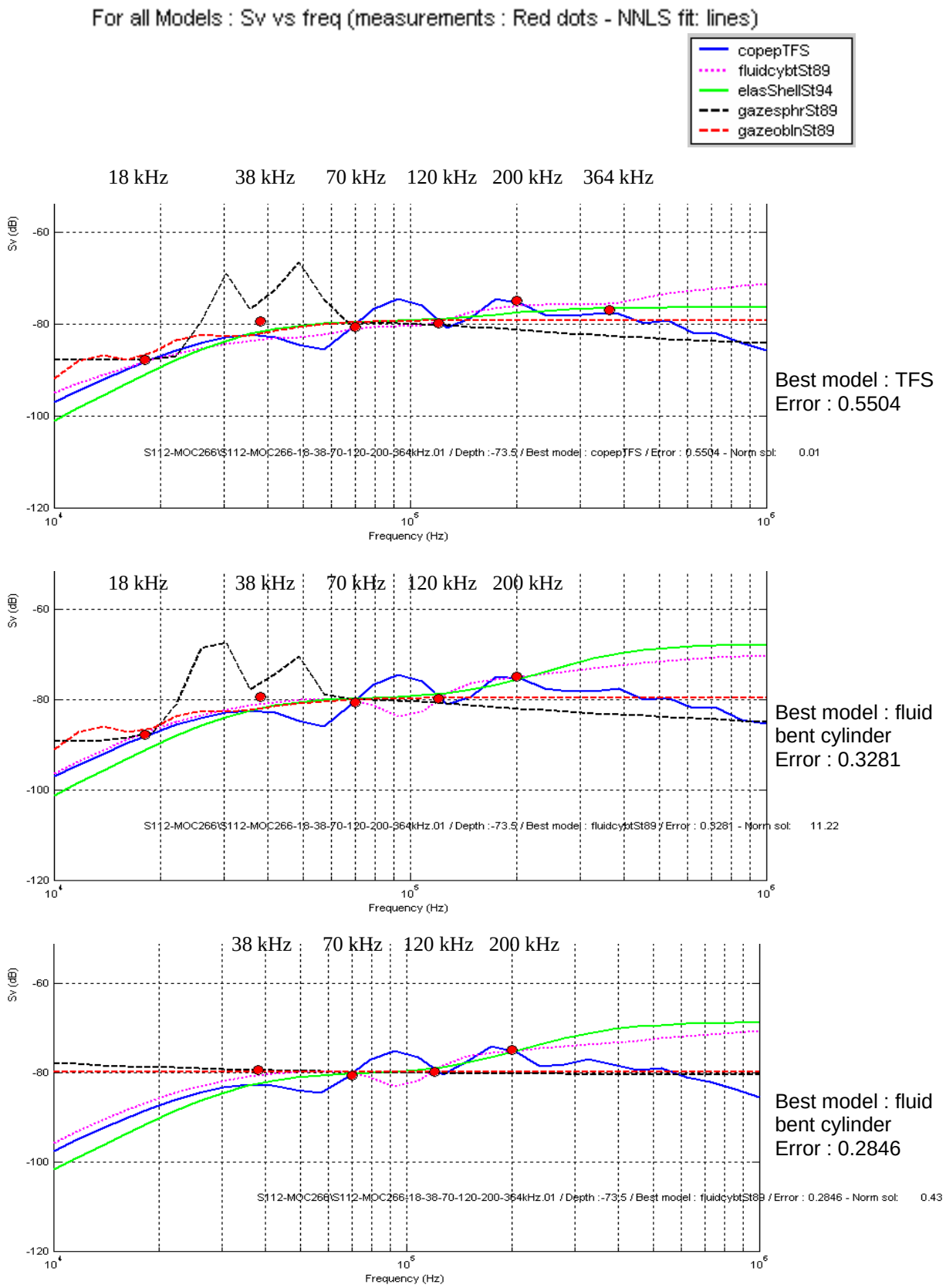

(a)

Figure 12. Differences in the model recognition according to the frequencies involved on two examples: processing with the six frequencies (top), with the four middle frequencies (bottom), without 364 kHz (a-middle) or without 18 kHz (b-middle).

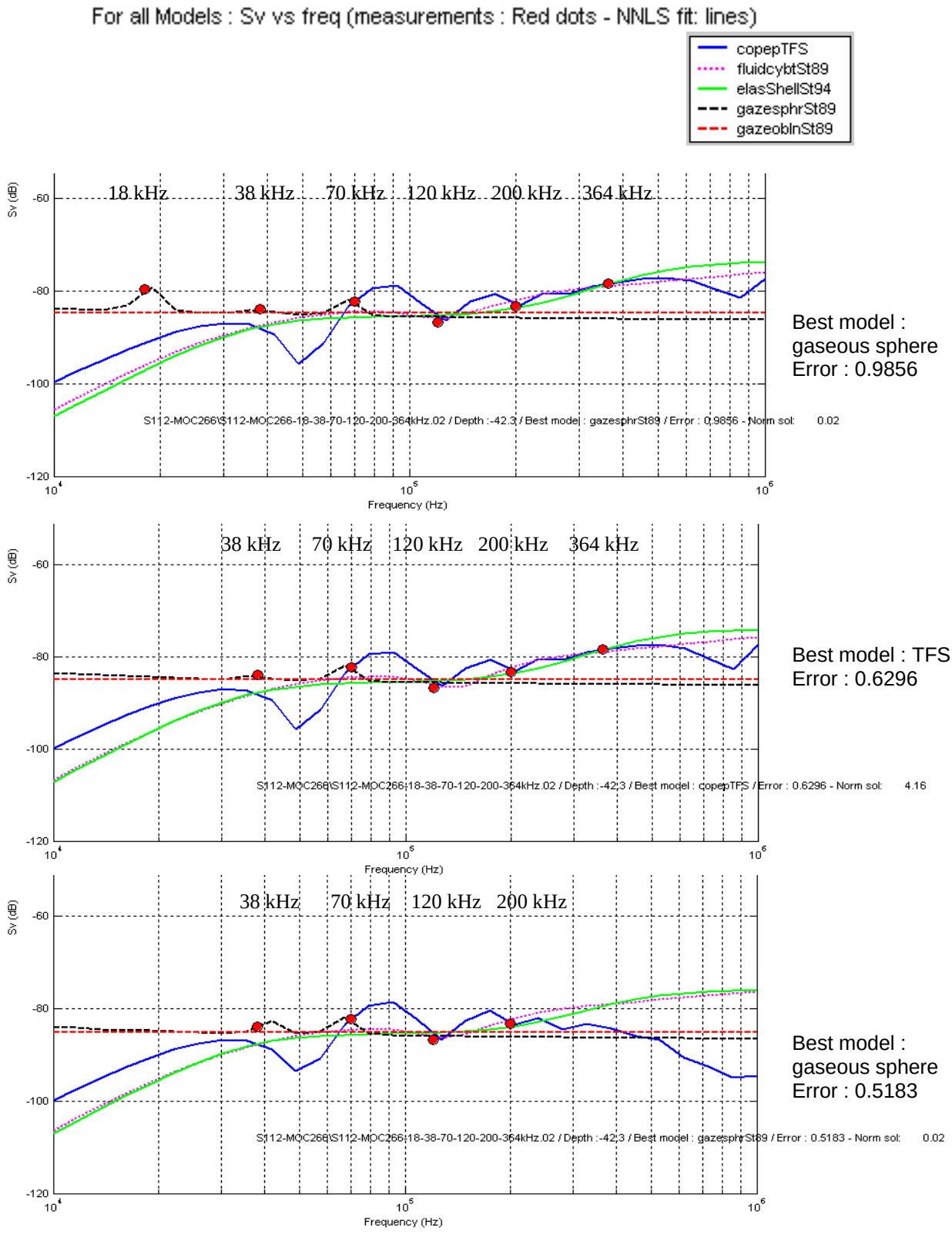

(b)

Figure 12. Differences in the model recognition according to the frequencies involved on two examples: processing with the six frequencies (top), with the four middle frequencies (bottom), without 364 kHz (a-middle) or without 18 kHz (b-middle).

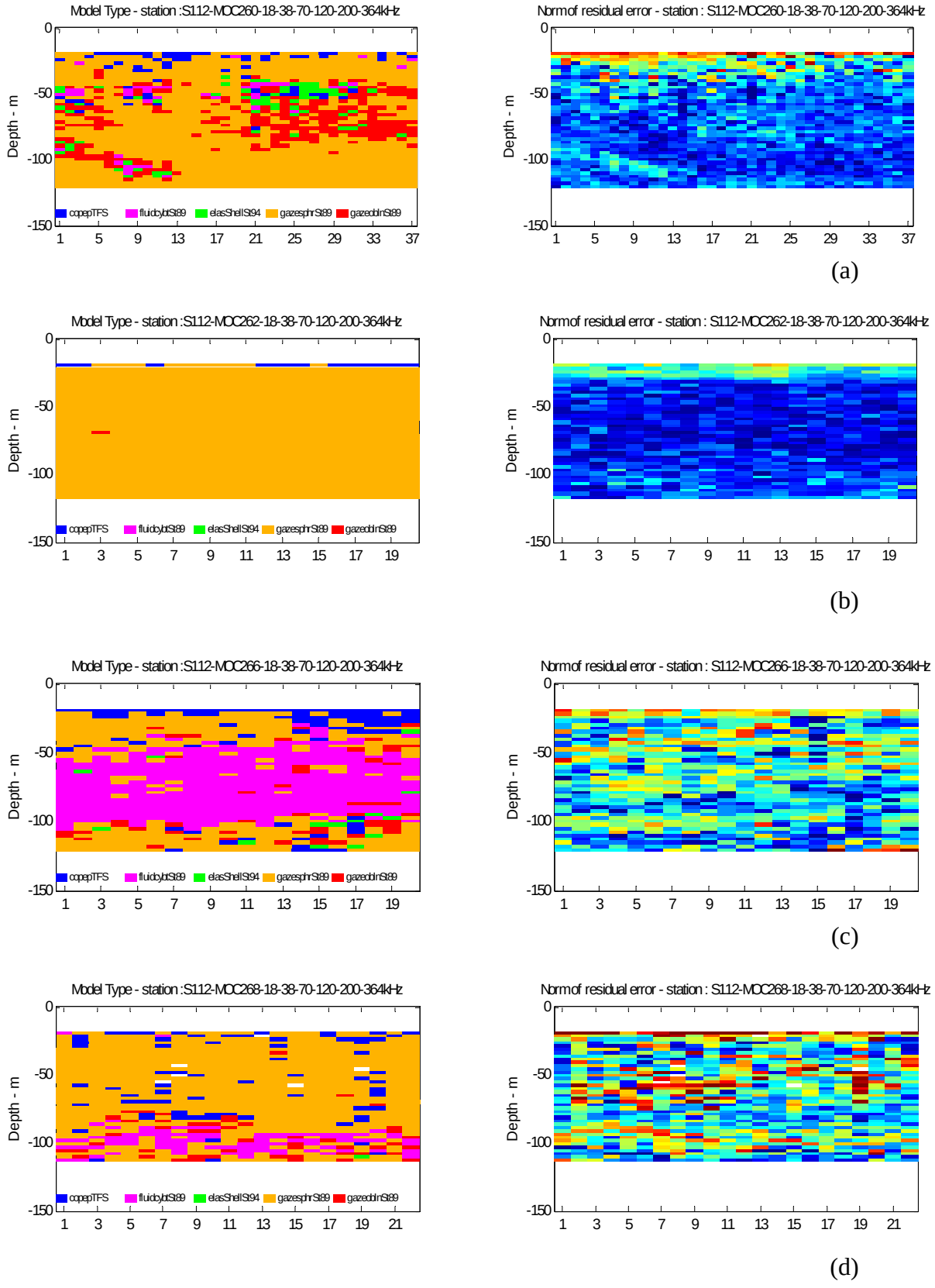

Figure 13. Results of the processing without 18 nor 364 kHz for the Mocness stations 260(a), 262(b), 266(c) and 268(d): models (left)-norm of residual error (right).

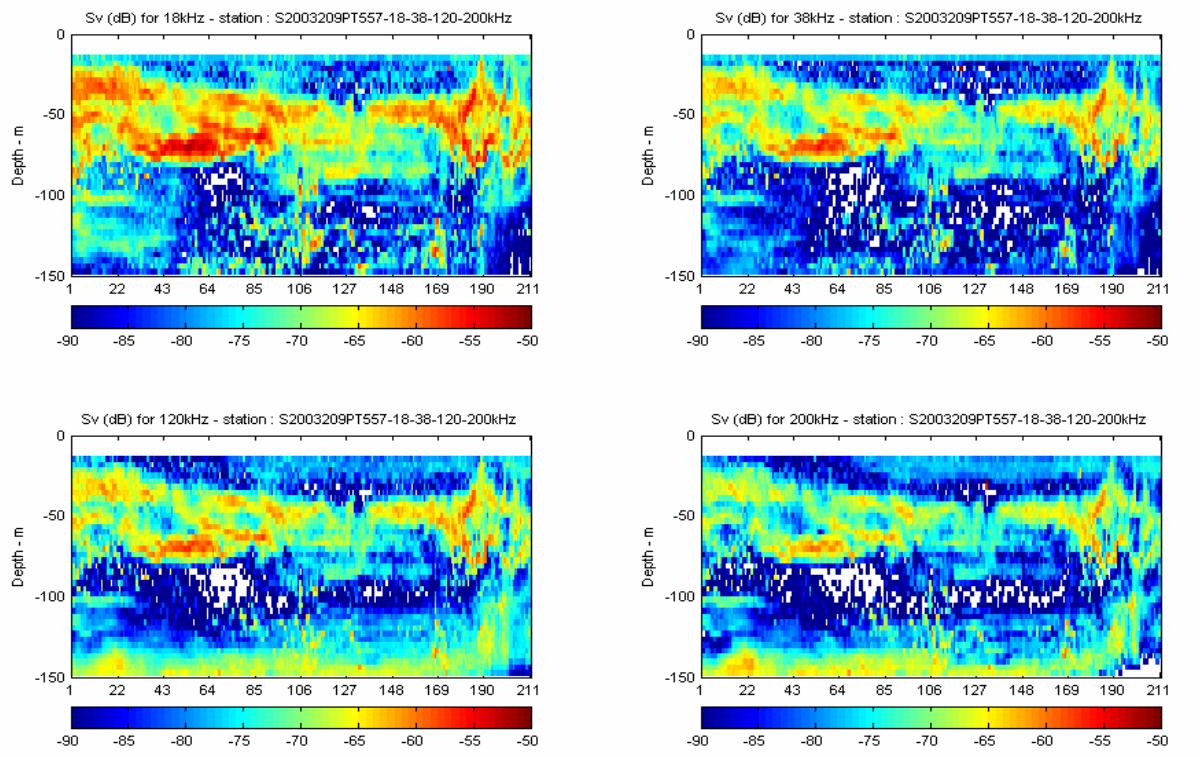

Figure 14. Echograms at the four frequencies 18, 38, 120 and 200 kHz corresponding to the pelagic trawl 557 during the Survey 209 in 2003. Catch between 110 and 124 meters deep was 45 kgs of krill, 7kgs of polar cod and 7 kgs of 0-polar cod.

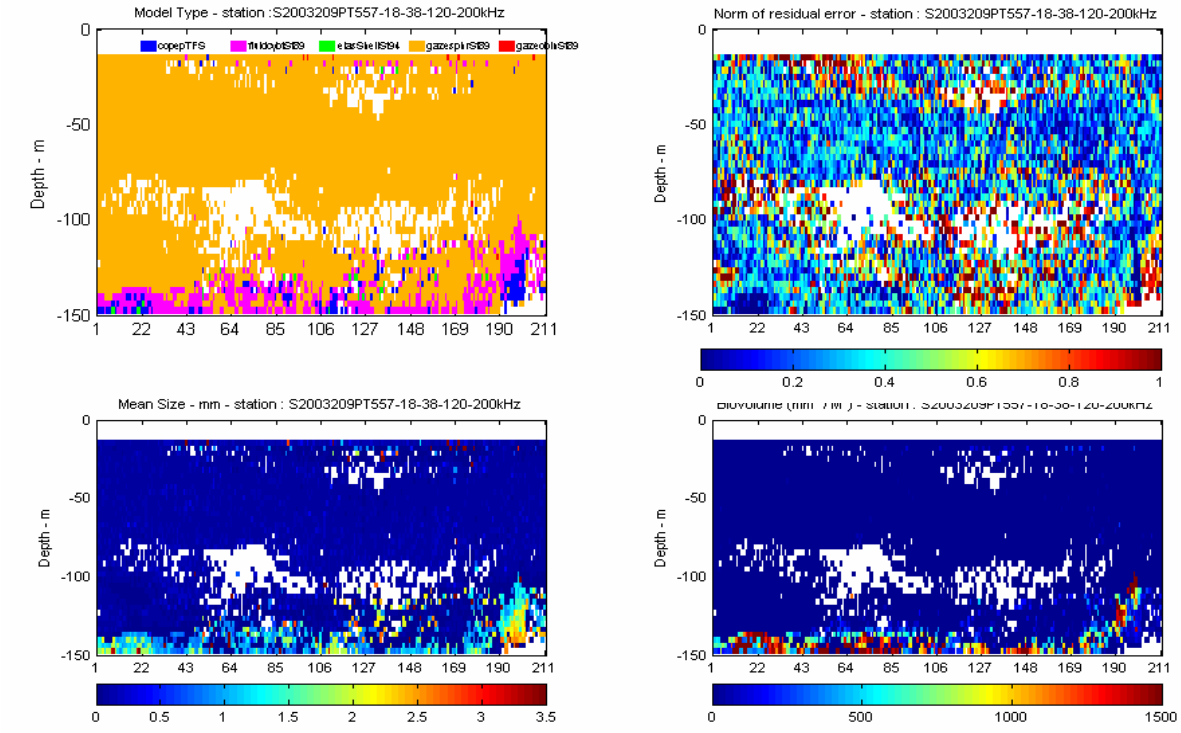

Figure 15. Result of the classification processing with the five models available and a size range of [0.05 10] mm. Legend for the models:

TruncFldSph HPFlBentCyl HPElasShell HPGasSphere HPGasProlSphd

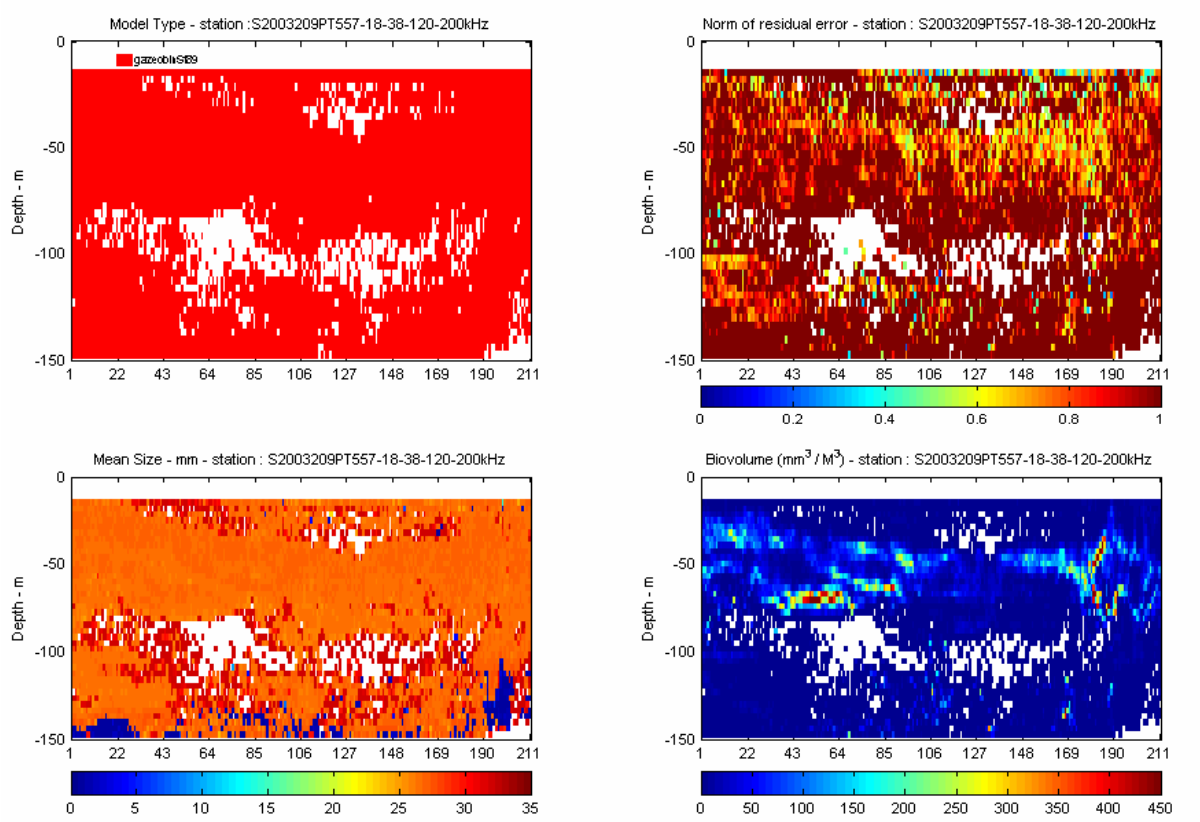

Figure 16. Result of the processing with only the gaseous prolate spheroid model available and a size range of [1 30] mm.